Sell when you can, you are not for all markets

9. PLASTIC ELECTRONICS

For the principles of semiconductor devices (ref: D) : http://ece-www.colorado.edu/~bart/book/book/

Sources
No Spec: Text
W: Wikipedia
D: web above

Schottky Barrier

- Formed when $\Phi_m > \Phi_s$ for n-type semiconductor
- Upon contact, electron depletion region of width W is formed
- Contact potential: $V_0 = (\Phi_m - \Phi_s)/e$
- Schottky Barrier Height: $\Phi_B = \Phi_m - X = eV_0 + (E_c - E_{FS})$

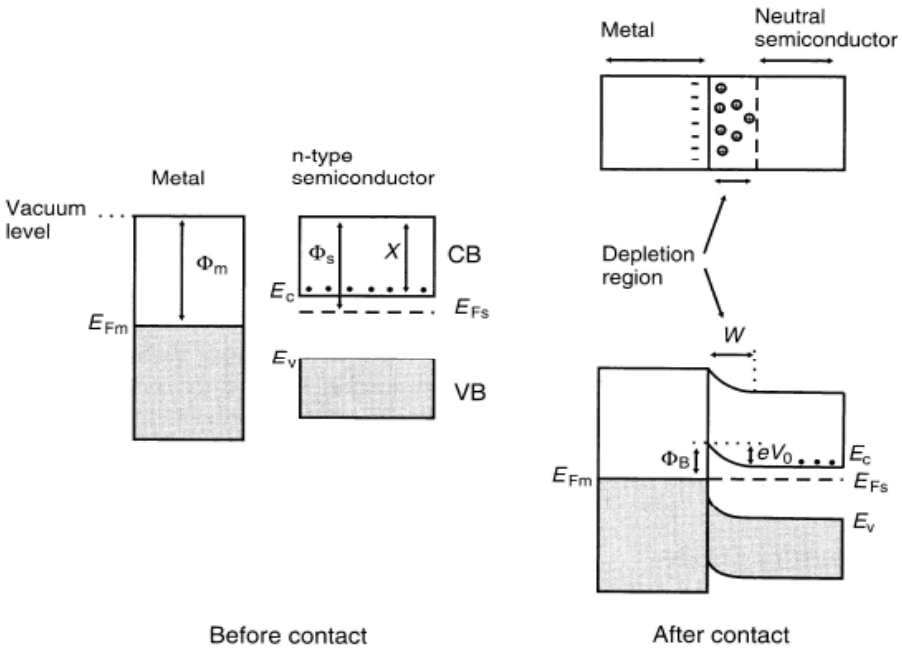

Figure 9.1 Formation of a Schottky barrier between a metal and an n-type semiconductor. CB and VB are the conduction and valence bands, respectively; E_c and E_v are the edges of the conduction and valence bands, respectively; E_{Fs} and E_{Fm} are the Fermi levels of the semiconductor and metal, respectively; Φ_s and Φ_m are the work functions of the semiconductor and metal, respectively; X is the electron affinity of the semiconductor; Φ_B is the Schottky barrier height; and V_0 is the contact potential.

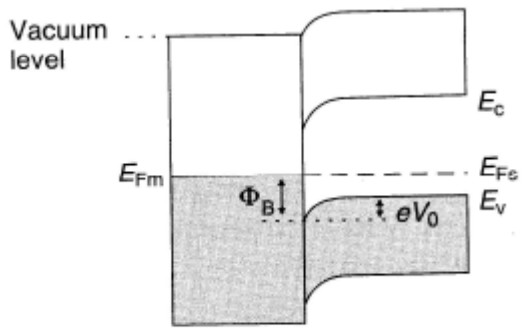

p-type semiconductor
Schottky barrier
When $\Phi_m < \Phi_s$

Schottky Diode

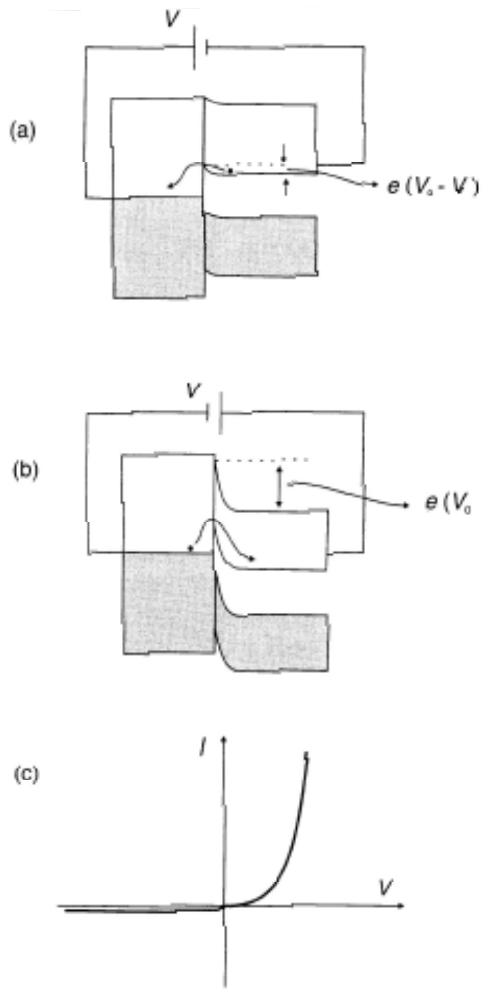

Figure 9.2 Schottky diode. (a) Bands in forward bias. (b) Bands in reverse bias. V is the applied voltage and V_0 is the contact potential. (c) Current I versus voltage V characteristics.

Forward Current

$$I = I_0[\exp(\frac{eV}{k_B T}) - 1]$$

where I_0 is a constant that is related to the barrier height of the MS junction

Reverse Current

small and due to the thermal emission of the electrons over the barrier Φ_B

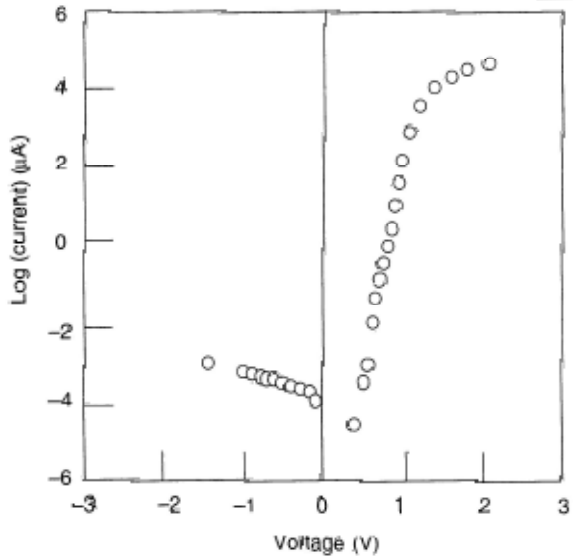

Figure 9.4 Current versus voltage characteristics for an In/polythiophene/Au diode. Reprinted from *Jpn. J. Appl. Phys.*, **33**, Kuo CS, Wakin FG, Sengupta SK, Tripathy SK, 'Schottky and metal–insulator–semiconductor diodes using poly(permission from the Japanese Society of A

Real Schottky Diode Forward Current

$$I = I_0 \exp(\frac{eV}{nk_B T})$$

where n is called the ideality factor (1~2 for Si)

n=3.8 for for Fig. 9.4

Schottky vs. Ohmic

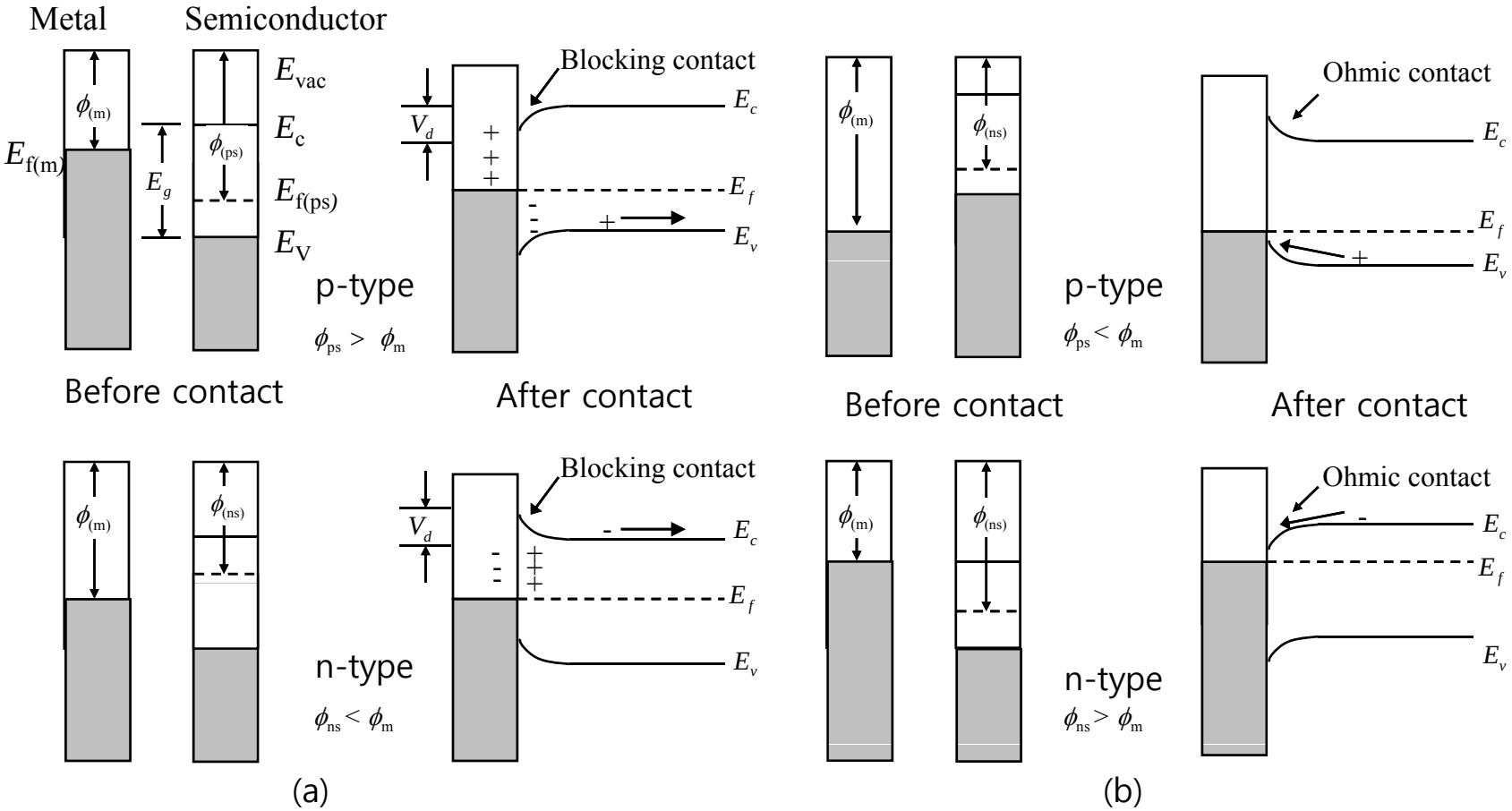

Band bending occurs in schottky barrier devices.(a) blocking contact formed when p- and n-type semiconductors make contact with metals with work functions less than or greater than those of semiconductors, respectively. (b) ohmic cantact formed when the work functions of metal are greater than (p-type) or less than (n-type) those of the semiconductor

- **For ohmic contact, I-V characteristics are linear and symmetric**
- **Practically, heavy doping of semiconductor at the interface region thus reducing W is used for preparing Ohmic contact**

MIS (MOS) Capacitor

- **Flat band** condition: no charges present in semiconductor – thus no band bending
- **Depletion** is caused by pushing the hole and leaving behind the localized acceptor anion
- **Inversion** layer is due to the minority carrier.

Ideal case
$\Phi_s = \Phi_m$

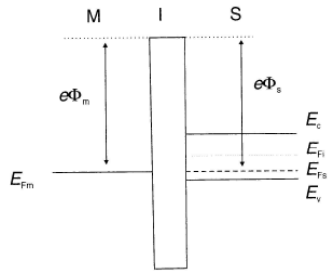

Figure 9.5 Energy band diagram for the ideal MIS structure based on a p-type semiconductor at zero applied bias. In this case, it is assumed that the work function of the semiconductor is equal to the work function of the metal ($\Phi_s = \Phi_m$). E_c and E_v are the edges of the conduction and valence bands, respectively; E_{Fs} and E_{Fm} are the Fermi levels of the semiconductor and metal, respectively; and E_{Fi} represents the position of the Fermi level for intrinsic material.

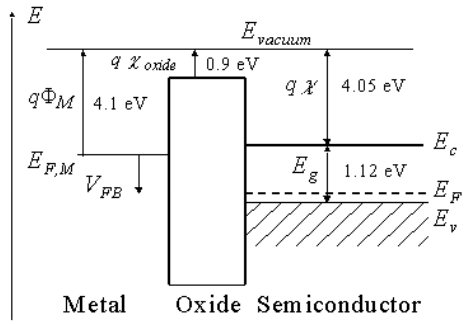

Figure 6.2.4: Flatband energy diagram of a metal-oxide-semiconductor (MOS) structure consisting of an aluminum metal, silicon dioxide and silicon.

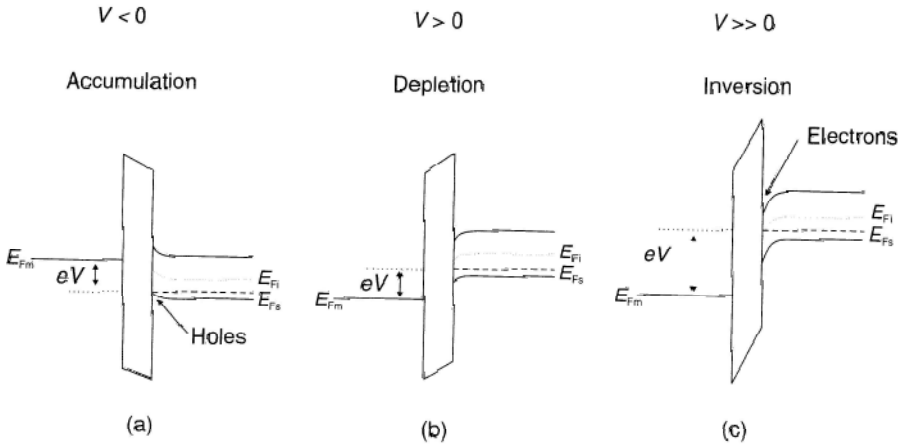

Figure 9.6 Energy band diagrams for an MIS structure based on a p-type semiconductor with different voltages applied to the gate electrode. (a) Negative voltage applied to gate, holes accumulate at semiconductor surface; (b) positive voltage applied to gate, depletion layer forms at semiconductor surface; (c) large positive voltage applied to gate, layer of negative charge (inversion layer) forms at semiconductor surface. V = applied voltage; E_{Fm} = metal Fermi level; E_{Fs} = semiconductor Fermi level; E_{Fi} = intrinsic Fermi level.

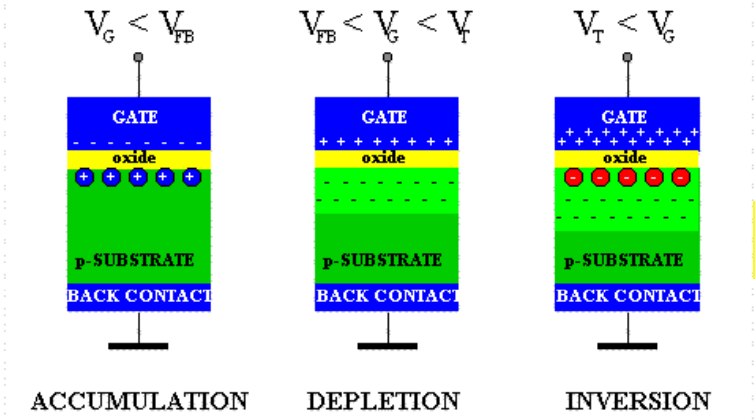

D

Organic MIS Structure

- The MOS structure is treated as a series connection of two capacitors: the capacitance of the oxide and the capacitance of the depletion layer.
- **Inversion layer** is due to the minority carrier. Therefore, slow response is observed in capacitance measurement; making it absent at high freq. measurement
- **Large hysteresis effects** are often observed due to the mobile ions, trapping of charges, and polarization of the insulating layer

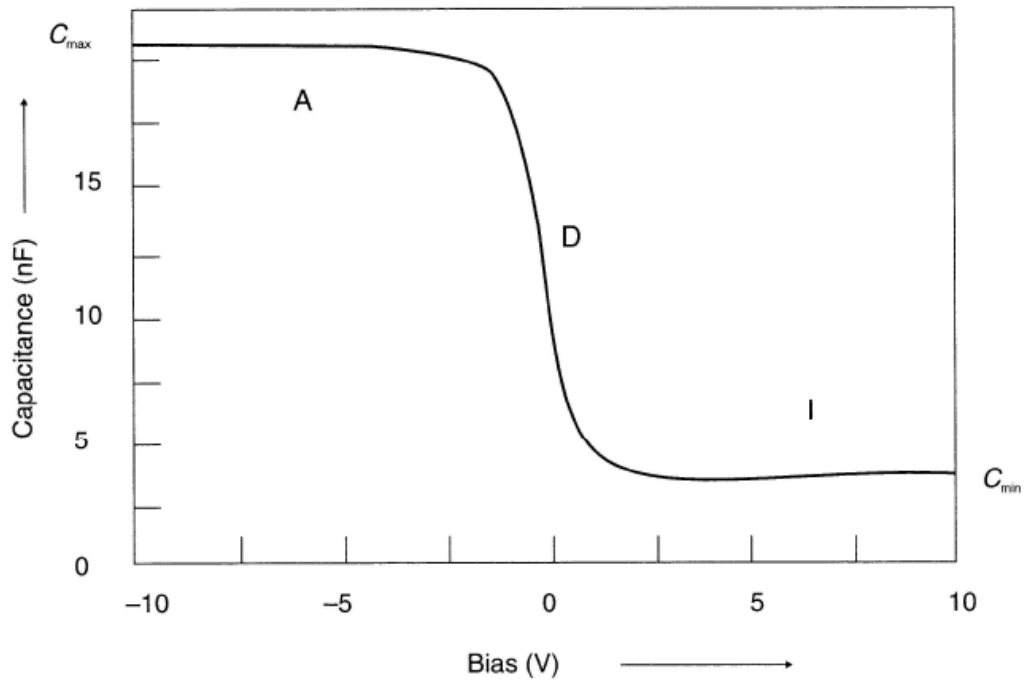

Figure 9.7 Capacitance versus voltage behaviour for an MIS structure comprising Si/SiO_2/polythiophene/Au measured at 111 Hz and at 270 K. The accumulation A, depletion D and inversion I regions are indicated. Reprinted from *Synthetic Metals*, **146**, Grecu S, Bronner M, Opitz A, Brütting W,' Characterization of polymeric metal–insulation–semiconductor diodes; pp. 359–363, Copyright (2004), with permission from Elsevier.

Organic FET (OFET)

- **OFET** operates in the **accumulation region**
- **Grounded source electrode**

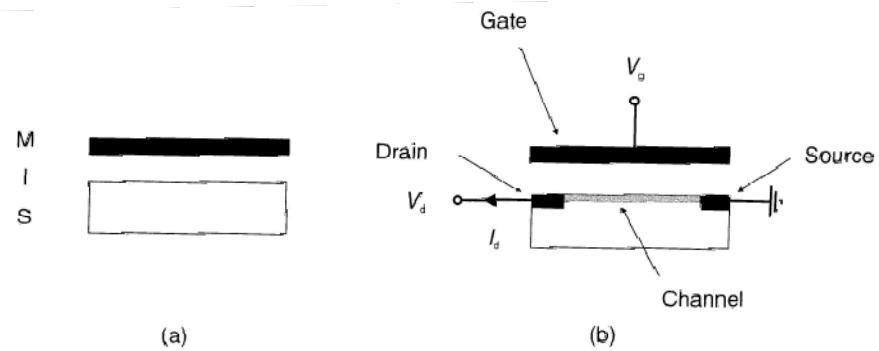

Figure 9.8 Contrast between (a) MIS structure and (b) MISFET.

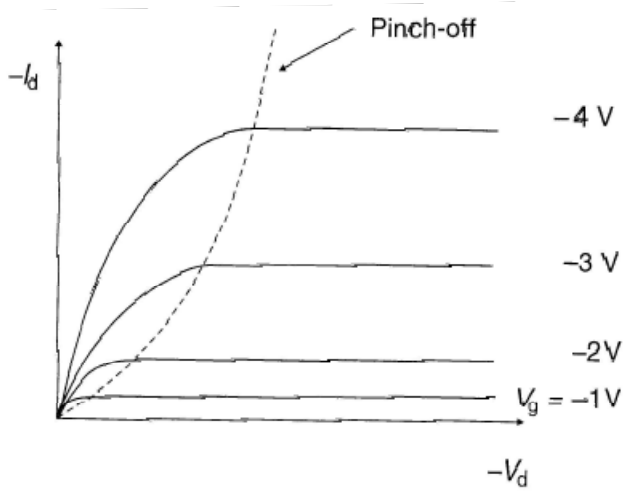

Lower V_d regime

$$I_d = \frac{WC_i}{L}\mu\left(V_g - V_t - \frac{V_d}{2}\right)V_d$$

Saturation Regime

$$I_d = \frac{WC_i}{2L}\mu\left(V_g - V_t\right)^2$$

Pinch-off

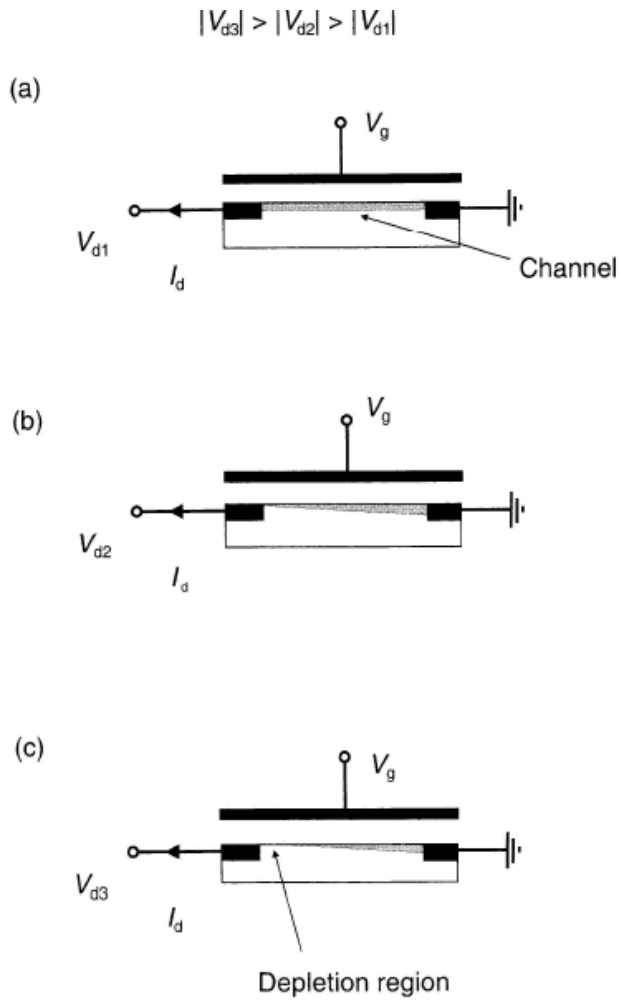

Pentacene

- $\mu = 0.3\ cm^2V^{-1}s^{-1}$
- Subthreshold swing of 1.6 V per decade
- On-off ratio : roughly 10^4

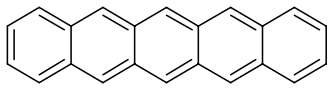

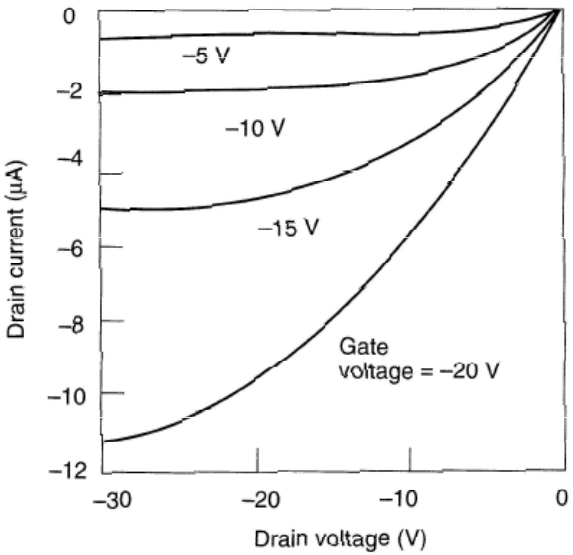

Figure 9.13 Drain current versus drain voltage characteristics of a MISFET based on pentacene. Device fabricated on a flexible polymer substrate. Gate dielectric: polyvinylphenol, thickness 270 nm. Reprinted with permission from Klauk H, Halik M, Zschieschang U, Eder F, Schmid G, Dehm C, *Appl. Phys. Lett.*, **82**, 'Pentacene organic transistors and ring oscillators on glass and on flexible polymeric substrates', pp. 4175–4177. Copyright (2003) American Institute of Physics.

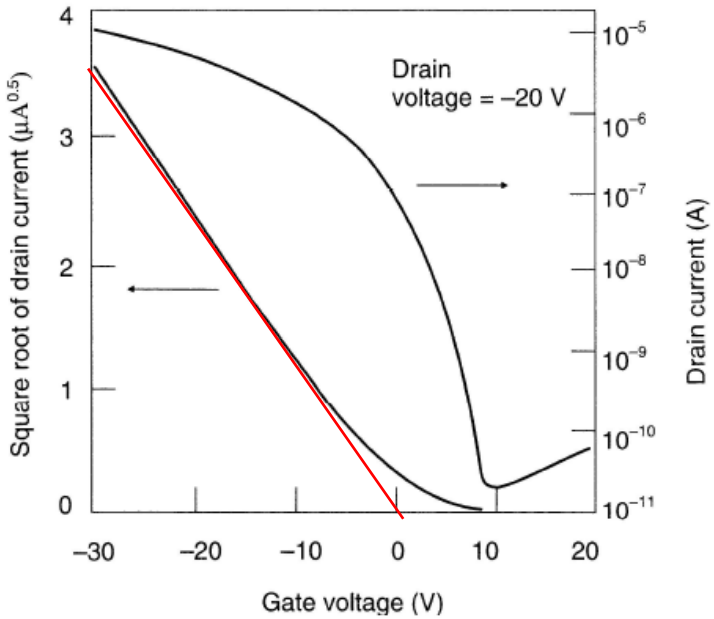

Saturation Regime

$$I_d = \frac{WC_i}{2L}\mu\left(V_g - V_t\right)^2$$

Plot $I_d^{1/2}$ vs Vg

Subthreshold Conduction is due to the conductivity of the organic semiconductor

Low Voltage Operating OFET

Marcus Halik, et. al, Nature, vol. 431, 963 (2004)

- **I_{on}/I_{off} ratio : 10^6**
- **Threshold voltage(V) : -1.3 V**
- **mobility : 1 $cm^2/V^{-1}s^{-1}$**

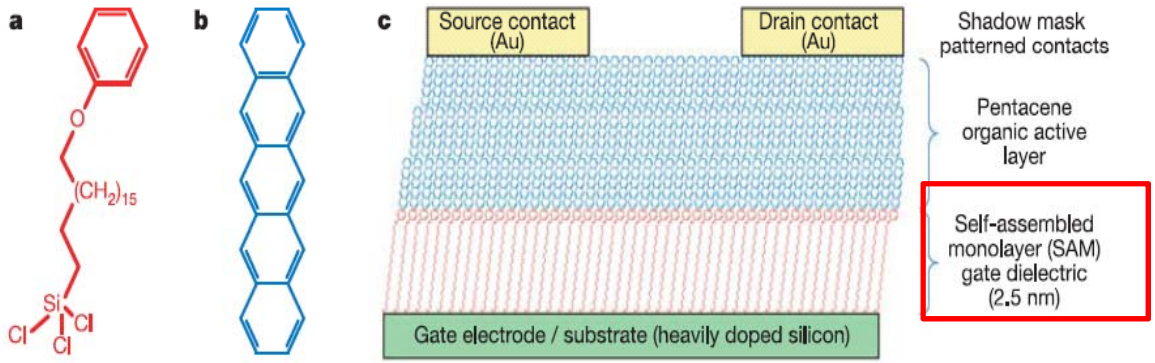

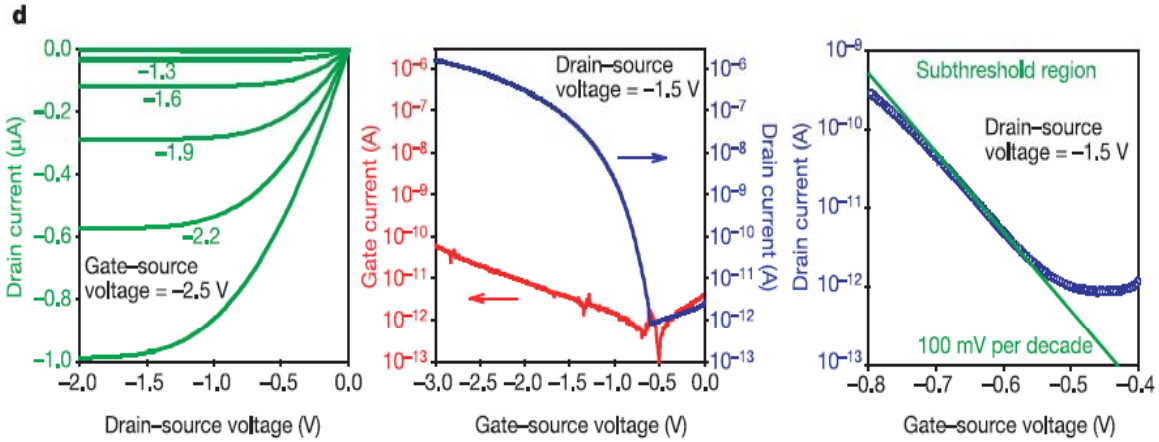

Controlling Carrier Density by SAM

***S. Kobayashi et al., Nature Materials* 3, 317 (2004)**

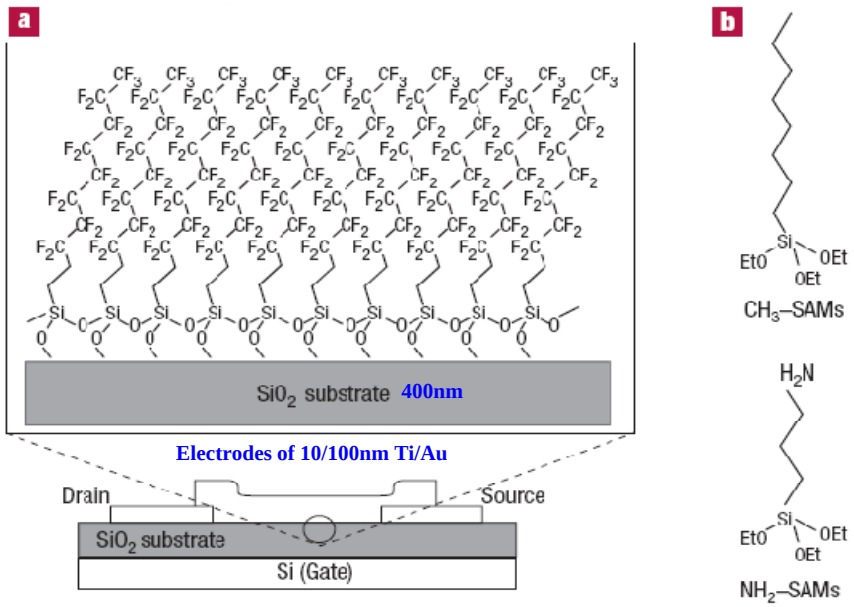

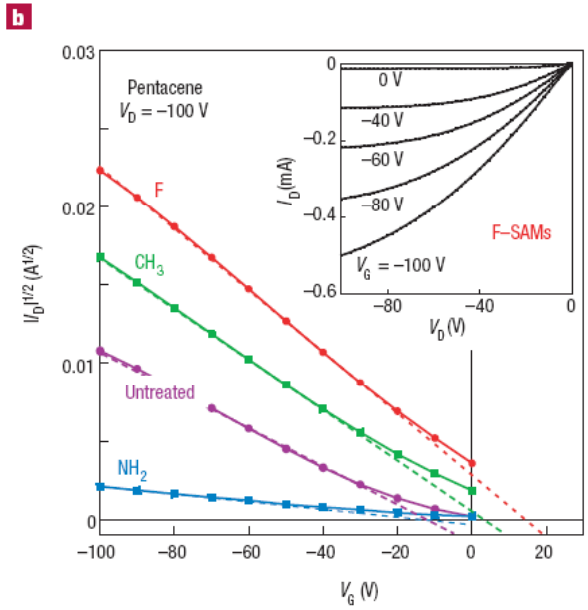

F-SAM brings about the accumulation of holes at the interface

Table 2 Field-effect mobility μ and threshold voltage V_{th} determined from Figs 3b and 4b for pentacene (p-type) and C_{60} (n-type) TFTs.

	Surface treatment	μ ($cm^2 V^{-1} s^{-1}$)	V_{th} (V)
Pentacene	F-SAMs	0.20	17
	CH_3-SAMs	0.13	5.0
	Untreated	0.086	−11
	NH_2-SAMs	0.0024	−11

OFET Semiconductors

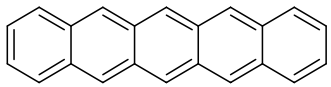

3 cm^2/V sec H. Klauk, M. Halik, U. Zschieschang et al., J. Appl. Phys. **92**, 5259 (2002).
7 cm^2/V sec 2003, SAIT.

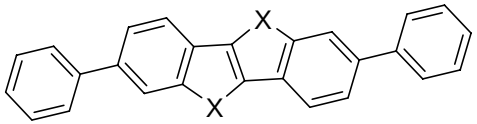

X=S : 2.0 cm^2/V sec (OTS)
X=Se : 0.3 cm^2/V sec

Kazuo Takimiya et. al. *J. Am. Chem. Soc.* **2006**, 128, 12604.

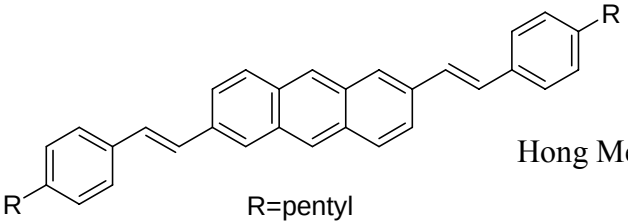

0.95 cm^2/Vs, on/off: 10^6

Hong Meng, et al**,** *J. Am. Chem. Soc.***; 2006,128, 9304.**

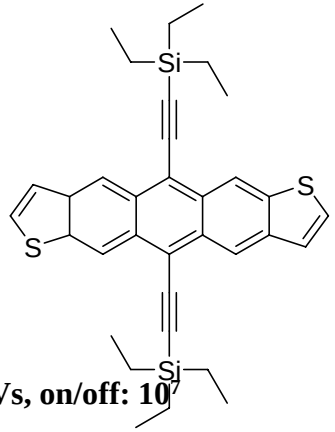

1.0 cm^2/Vs, on/off: 10^7

J. E. Anthony et al., *J. Am. Chem. Soc.,* **2005**, 127, 4986.

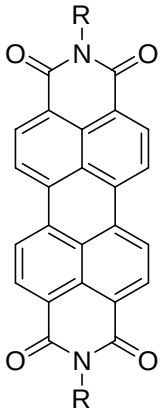

N-type
0.6 cm^2/V sec
P. R. L. Malenfant, et. al
Appl. Phys. Lett., **2002**, 80, 2517.

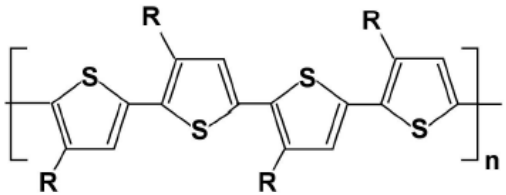

10^{-2} to 10^{-1} cm^2 V^{-1} s^{-1}

H. Sirringhaus et al., APL 77(3), 406 (2000)

W

Hand with the planned location of the RFID chip.

RFID tags used in libraries: square book tag, round CD/DVD tag and rectangular VHS tag.

RFID Tags

An RFID tag used for electronic toll collection.

- Passive Tag: lacks its own power source; small and implantable;
- Active Tag: smallest one is about the coin size
- Organic RFID: low cost, printable RFID

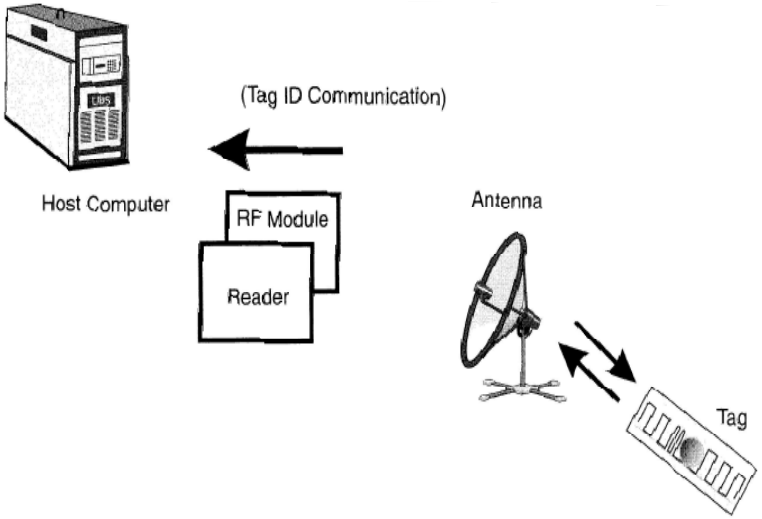

Figure 9.16 Schematic diagram of an RFID system. The antenna captures the tag ID number, analogue radiofrequency waves, then it is converted to digital information.

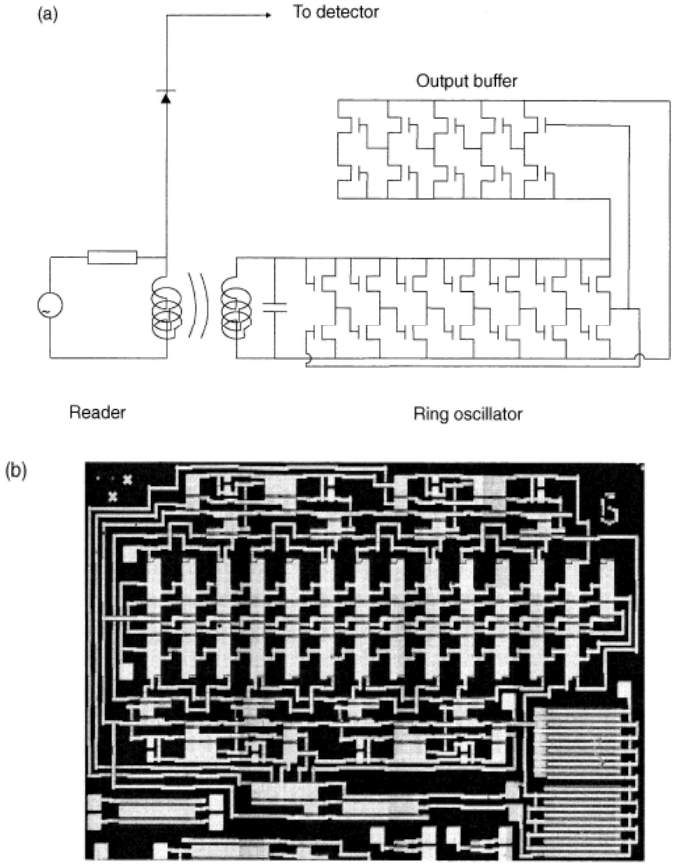

Figure 9.17 (a) Circuit diagram of a ring oscillator, fabricated using pentacene FETs. (b) Photograph of the organic integrated circuit. Reprinted with permission from Baude PF, Ender DA, Haase MA, Kelley TW, Muyres DV, Theiss SD, *Appl. Phys. Lett.*, **82**, 'Pentacene-based radio-frequency identification circuitry', pp. 3964–3966. Copyright (2003) American Institute of Physics.

OLED – Already, around us

LG storm

Samsung
SOUL

Sony 11-inch OLED, released in Japan at the end of 2007

KB bank
Electronic credit card

Iriver MP3P CLIX

Iriver PMP iAMOLED

Samsung
Kenox
NV24HD

Samsung & Germany
electronic passport

Why OLED?

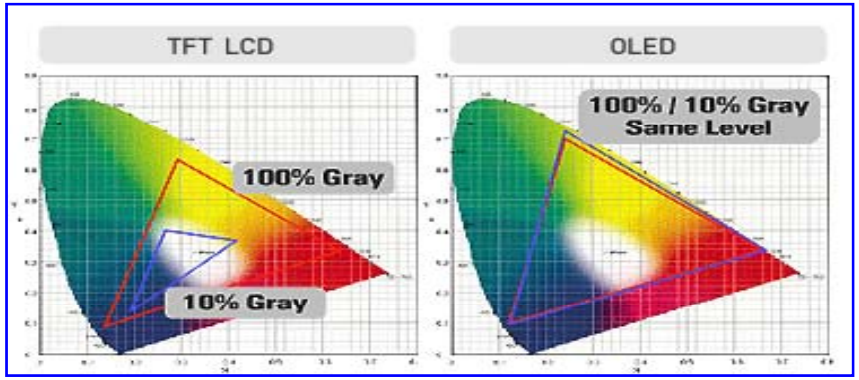

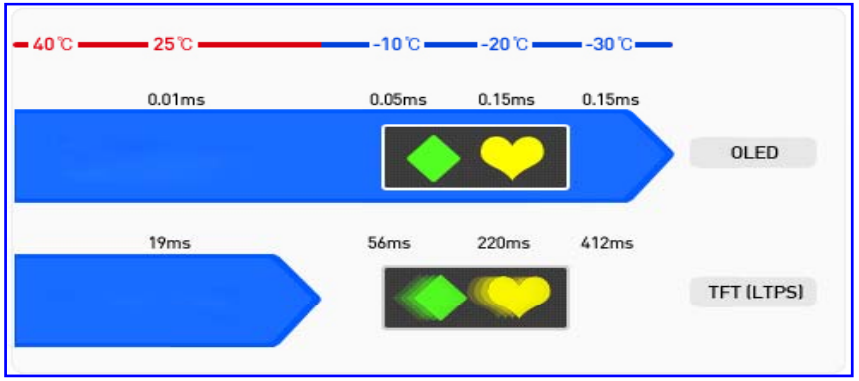

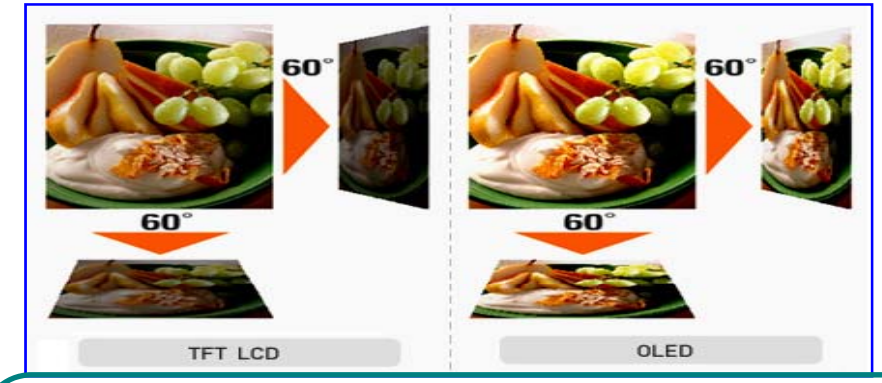

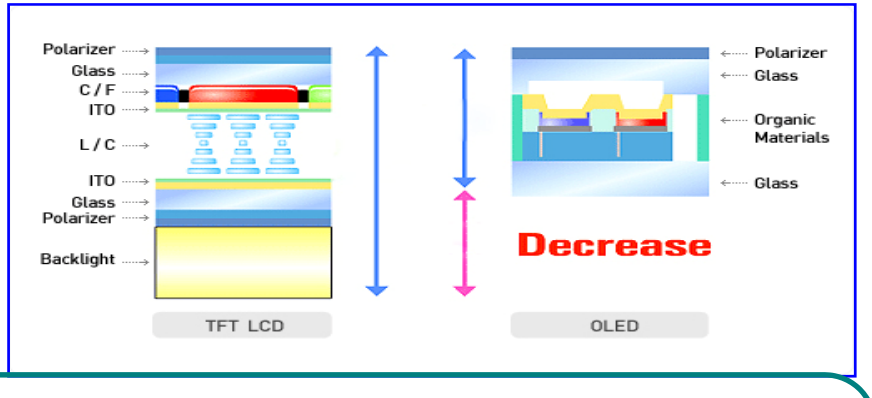

- **Superior viewing performance:** emissive bright colors, wide viewing angle, fast response time, and high contrast
- **Simple fabrication processes** vacuum deposition, inkjet printing, spin coating, roll-to-roll processing
- **Excellent operating characteristics** low operating voltage, power efficient
- **Good form factor** Flexible → Ultimate Portable Communication Devices

http://www.samsungsdi.co.kr

OLED Fundamentals

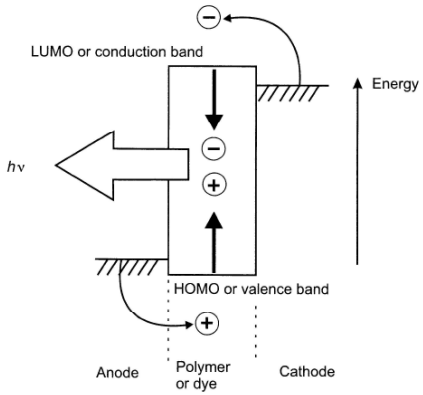

Figure 9.18 Schematic energy band structure of an organic light emitting device (OLED). The recombination of electrons and holes results in the emission of light of frequency ν and energy $h\nu$.

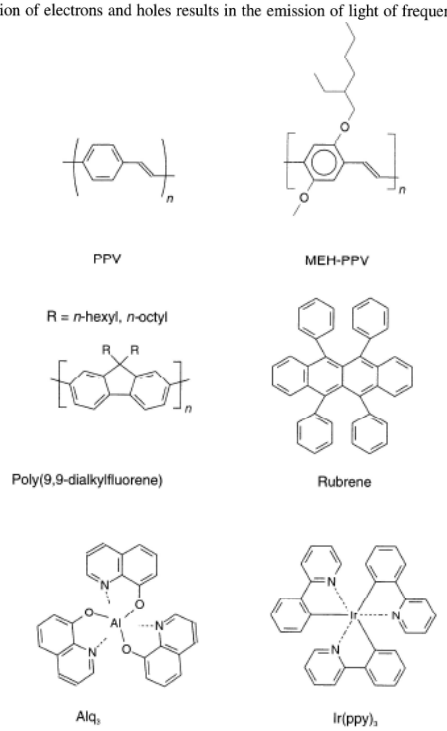

Figure 9.19 Organic compounds used as the emissive layer in OLEDs.

- **Luminescent entities**: small molecule, polymer, fluorescence or phosphorescence : Fabrication issues
- h & e recombination generating **exciton** (triplet & singlet)
- **Encapsulation** against water and oxygen

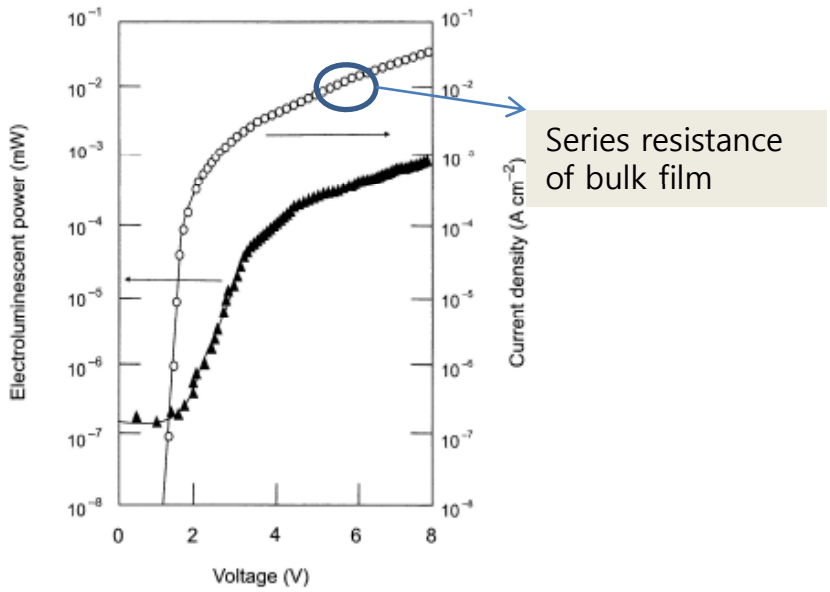

Figure 9.20 Current versus voltage and electroluminescence output versus voltage characteristics for an ITO/MEH-PPV/Al OLED. Reprinted with permission from Karg S, Meier M, Riess W, *J. Appl. Phys.*, **82**, 'Light-emitting diodes based on poly-*p*-phenylene-vinylene: I charge-carrier injection and transport', pp. 1951–1966. Copyright (1997) American Institute of Physics.

- **Schottky barrier type** OLED (above)
- SCLC Conduction
- Fowler –Nordheim Conduction

Color & Efficiency of OLED

- CIE chromaticity diagram
- White (0.31,0.32)
- Efforts to develop RGB & W

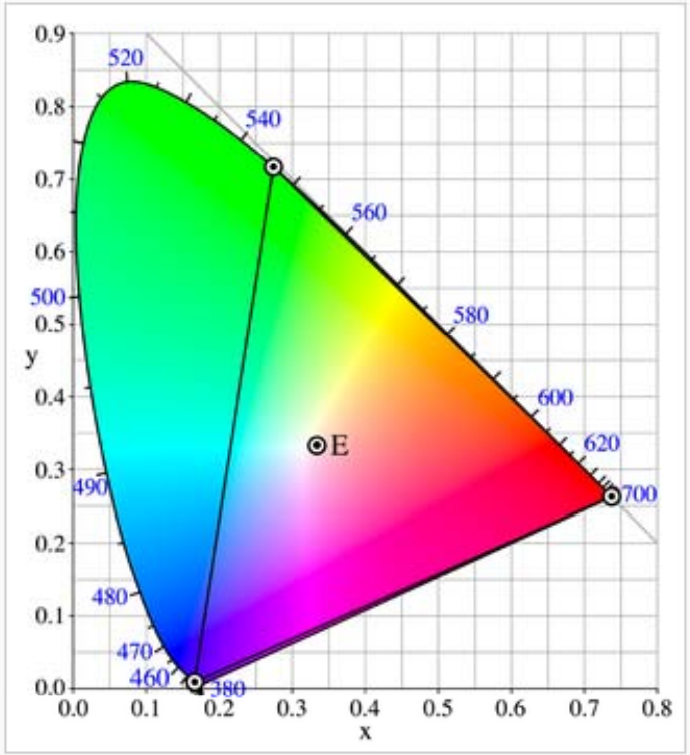

Gamut of the CIE RGB primaries and location of primaries on the CIE 1931 *xy* chromaticity diagram.

- **Photometric units** are used
- **cd m^{-2}** (read as nits) : computer screen (100 cd m^{-2}), average clear sky (8000 cd m^{-2})
- 1W 555 nm light (683 lm) while 1 W 700 nm light (27 lm)
- **External quantum efficiency**: ratio of the number of photons **emitted into the viewing direction** to the number of electrons injected
- **Internal quantum efficiency** : ratio of the total number of photons emitted to the number of electrons injected
- **Luminous efficiency**: cd A^{-1}
- **Luminescence power efficiency**: lm W^{-1}

Table 9.1 Common photometric units.

Property	Description	Units
Energy	Total amount of light emitted from source	Joules (J)
Luminous flux	Rate of energy emitted from source	Lumen (lm)
Luminous intensity	Flux emitted from a point source per unit solid angle	Candela (cd) ≡ lumens per steradian (sr)
Luminance	Flux emitted per unit surface area of extended source per unit solid angle	cd m^{-2}

Table 9.2 Performance of polymer-based organic light emitting devices (Sumation Co. Ltd, 2006) [28].

Colour	Voltage (V)	Luminous efficiency at 400 cd m^{-2} (cd A^{-1})	Luminous power efficiency at 400 cd m^{-2} (lm W^{-1})	Measured lifetime at room temperature at fixed luminance (h) at [cd m^{-2}]	Extrapolated lifetime at 100 cd m^{-2} at room temperature (h)
Phosphor red	6.5	10.6	5.1	512 at 4029	800 000
Fluorescent red	3.6	2.3	2.0	936 at 3000	300 000
Green	4.9	15.8	10.1	320 at 6000	500 000
Blue	5.5	9.6	5.5	619 at 1800	200 000
White	6.8	4.5	2.1	474 at 1440	65 000

All data taken using common cathode and may include an interlayer.

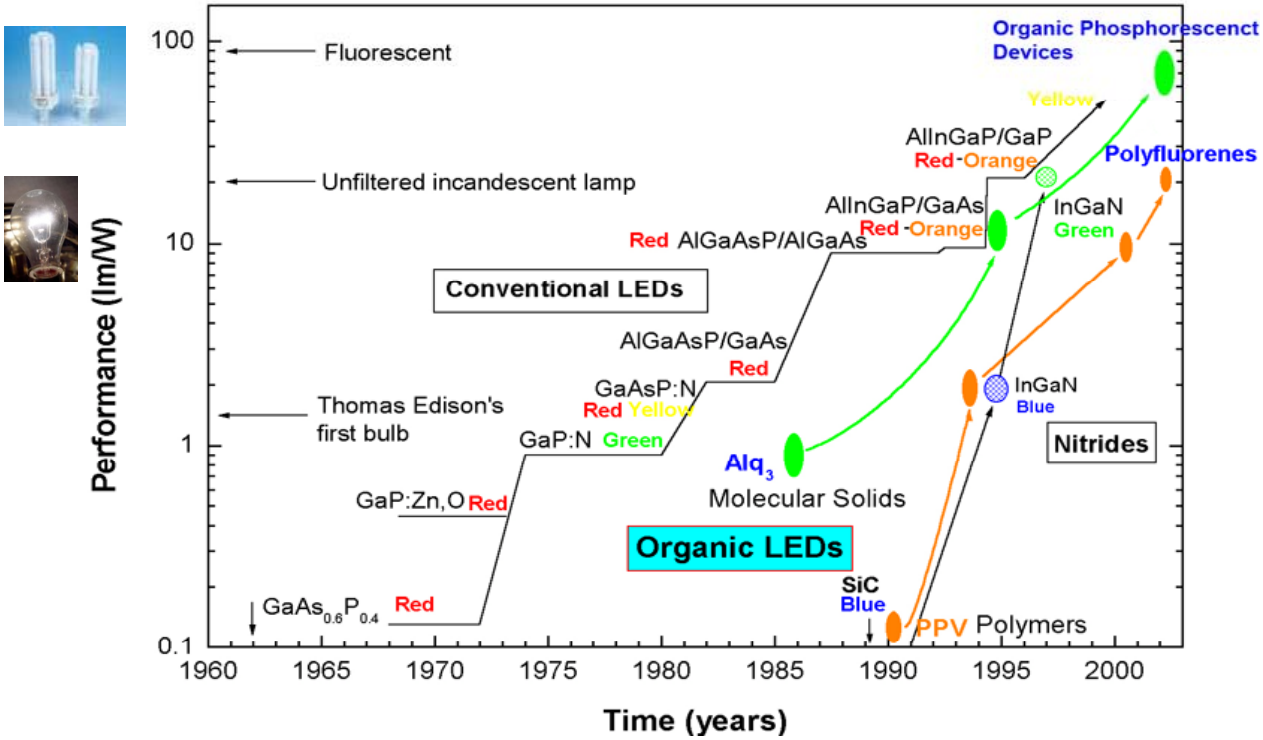

Data added to the original plot of J. R. Sheats *et al.*, Science 273, 884 (1996)

Practical OLED: Multi-layers

- **PEDOT modified anode**: surface smoothing and adhesion promoting
- **LiF** or organic monolayer **modified cathode**: improve electron injection via band bending
- **Carrier transport layers** are open doped: p-type dopant F4-TCNQ, n-type dopant Li or Cs (p-i-n device)

Enhanced device efficiency & lifetime via multi-layering

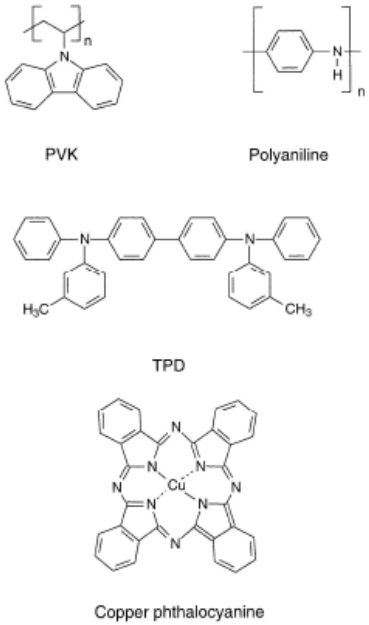

Figure 9.22 Hole-transporting molecules used in OLEDs.

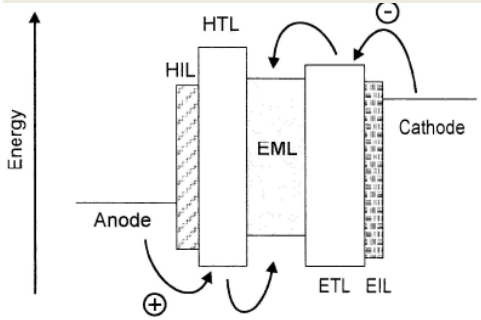

Figure 9.24 Multilayer OLED. HIL, hole injection layer; HTL, hole transport layer; EML, emissive layer; ETL, electron transport layer; EIL, electron injection layer.

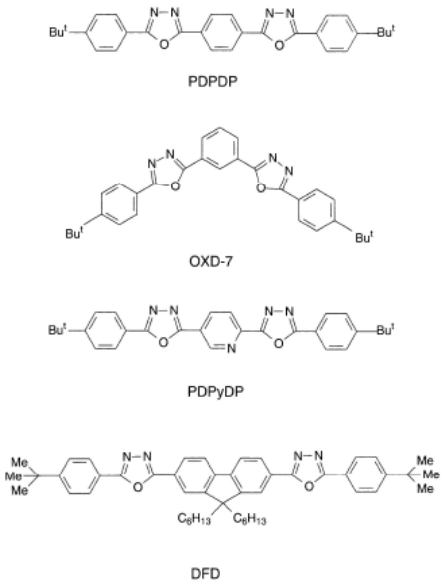

Figure 9.23 Electron-transporting molecules used in OLEDs.

ITO / 2-TNATA(60nm)/ NPB(20nm) / P-DAC(40nm) / Alq3(20nm) / LiF(1nm) / Al(100nm)

PhoLED

- Use of both the **singlet & triplet** excitons to give very high EL efficiency
- Luminescence **lifetime** is in the order of μs

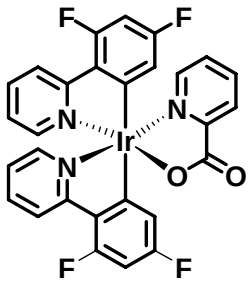

C. H. Chen et al. *Adv. Mater*. **2005**.*17*. 285

EQE 14.4 %

ITO/NPB/Host:**Ir**/TPBI/LiF/Al

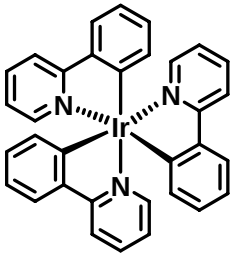

J. Salbeck et al. *Appl. Phys. Lett.*. **2004**.*85*. 3911

EQE 19.3 %

ITO/MeO-TPD:F4-TCNQ/spiro-TAD/TCTA:TAZ:**Ir**/BPhen/n-Bphen /Al

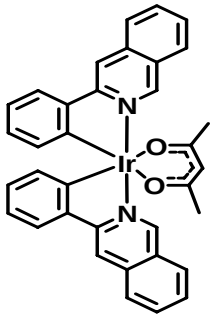

K. Meerholz et al. *Adv. Mater.*. **2006**.*18*. 948

EQE 10.8 %

ITO/PEDOT:PSS/HTL/PVK: PBD:**Ir**/CsF/Al

Y. You and S. Y. Park *et al.*, *J. Mater. Chem.* **2006**, *16*, 4006

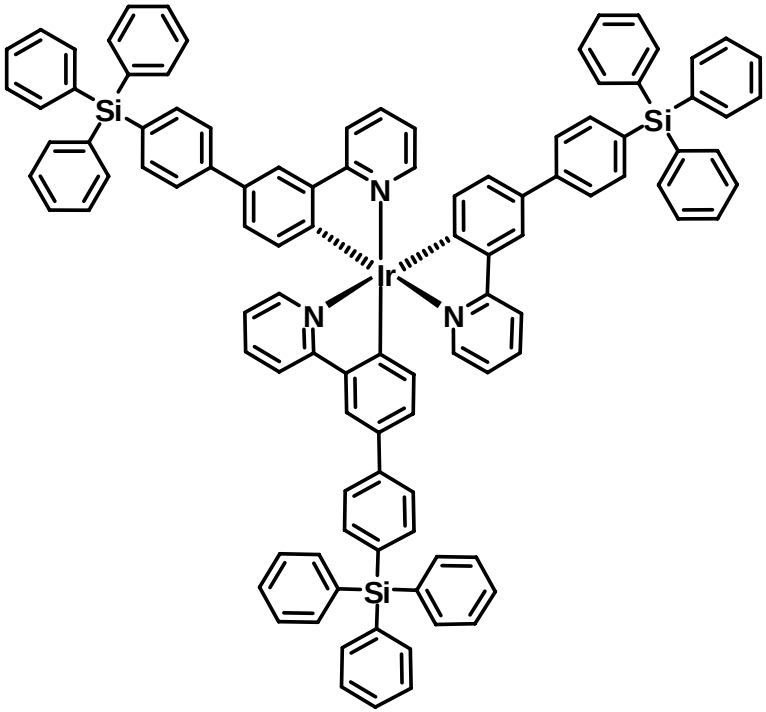

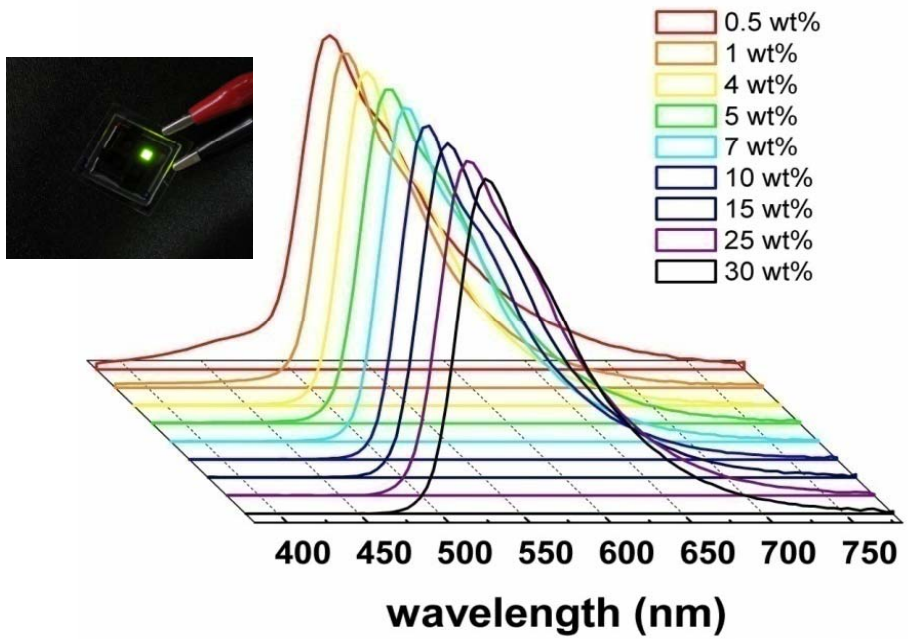

electrophosphorescence

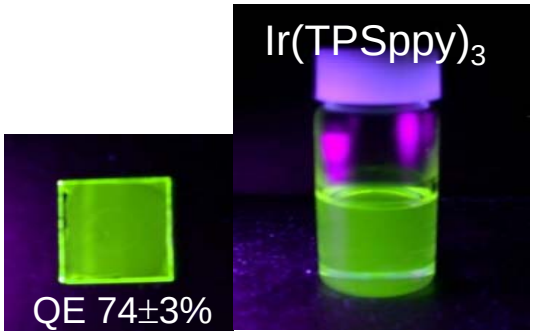

ITO/PSS:PEDOT/PVK:Ir/BCP/Alq_3/LiF:Al

Max luminance : 21250 cd/m^2
Max η_L : 32.8 cd/A (10 wt% doped)

For $Ir(ppy)_3$-doped reference device
Max luminance : 9432 cd/m^2
Max η_L : 26.4 cd/A (6 wt% doped)

OLED on Shaped Substrates

- Use of **glass mesa** increases the external efficiency by the factor of four (cf. critical angle of glass-air interface is 19°)

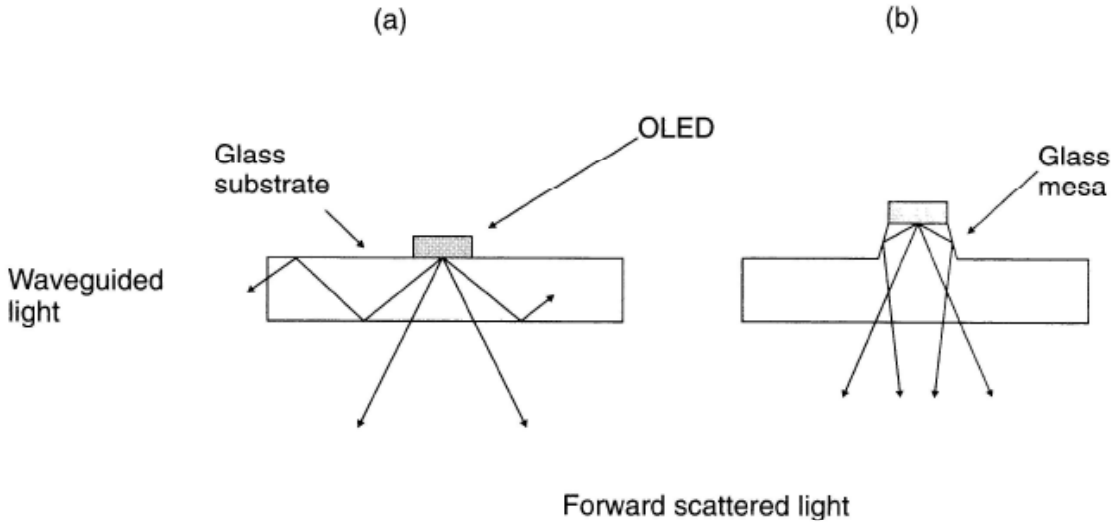

Figure 9.25 Schematic cross-section (not to scale) of an OLED fabricated on a shaped substrate (mesa) designed to increase the proportion of light emitted by the OLED in the forward direction. (a) Much of the emitted light is waveguided in the glass substrate and lost. (b) Most of the waveguided light is directed into the viewing direction by internal reflection from the walls of the glass mesa. From *IEEE Trans. Electron Dev.* **44**, Burrows PE, Gu G, Bulović Shen Z, Forrest SR, Thomson ME, 'Achieving full-colour organic light-emitting devices for lightweight, flat-panel displays', pp. 1188–1202, Copyright (1997) Reproduced by permission of IEEE.

Microcavity OLED Structure

- **Dielectric alternating stack** of SiO_2 (n=1.4) and TiO_2 (n=2.3) providing $\lambda/4$ thickness

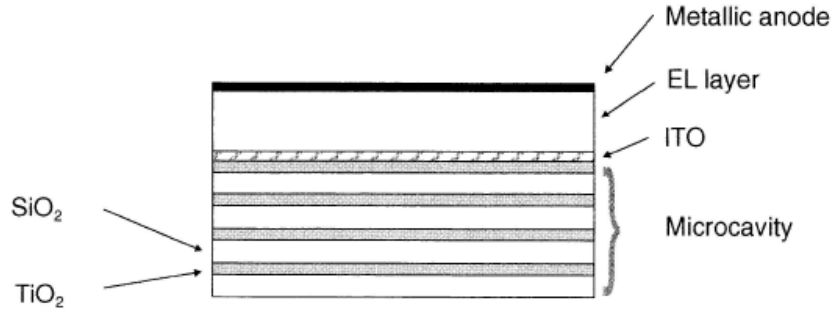

Figure 9.26 Organic light-emitting device fabricated on an optical microcavity.

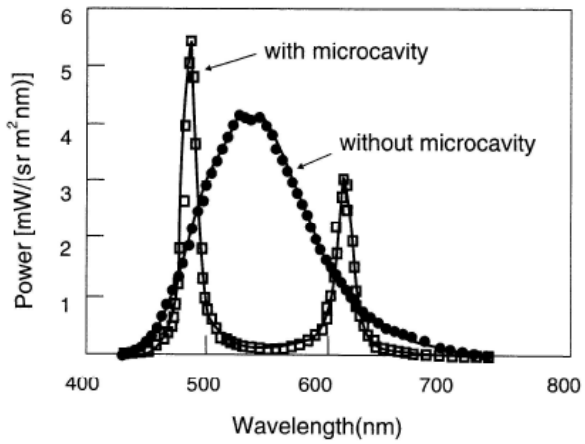

Figure 9.27 Electroluminescent output for an Alq_3 OLED fabricated on a microcavity compared to a reference device. Reproduced from *Organic Electroluminescent Materials and Devices*, T Nakayama, p. 365, Copyright (1997), with permission from Taylor & Francis Group LLC.

Single Blend Layer OLED

- MEH-PPV: DFD ratio change
- 100 times more efficient than that of pure MEH-PPV

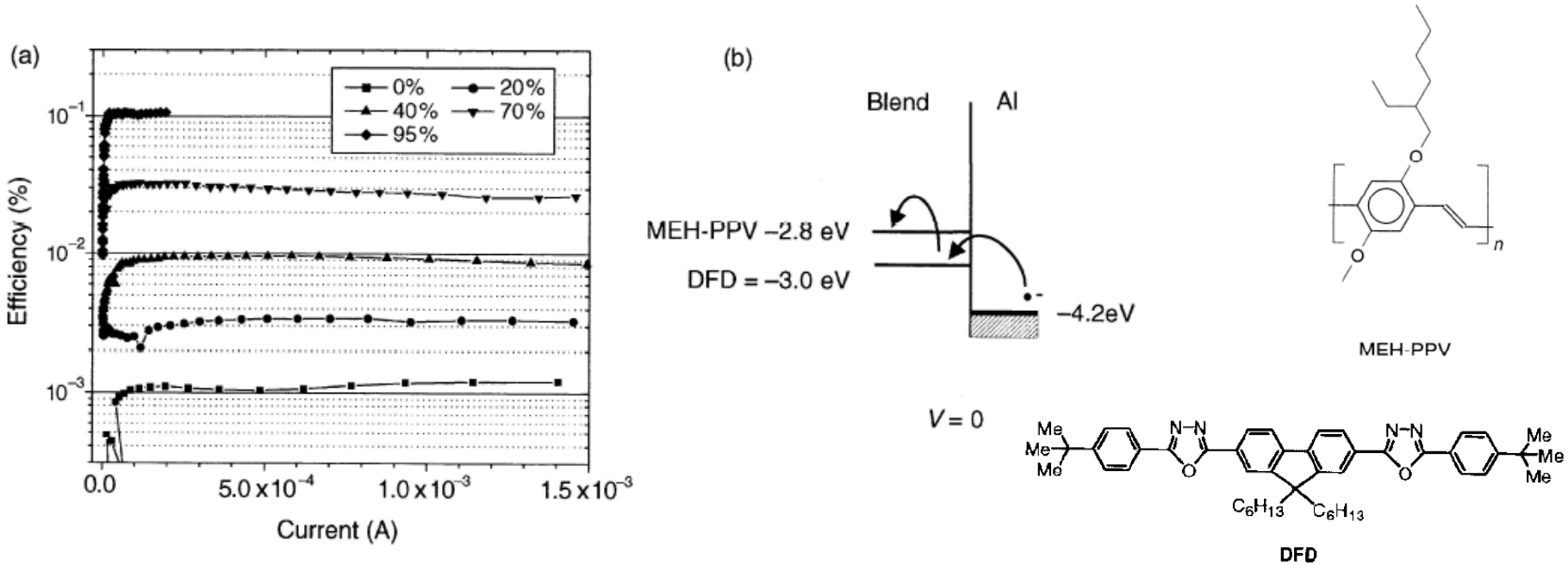

Figure 9.28 (a) External quantum efficiency versus current for OLEDs fabricated with MEH-PPV/DFD blended layers using blends with various concentrations (by weight) of DFD, an electron acceptor. Reprinted with permission from Ahn JH, Wang C, Pearson C, Bryce MR, Petty MC, *Appl. Phys. Lett.*, **85** 'Organic light-emitting diodes based on a blend of poly[2-(2-ethylhexyloxy)-5-methoxy-1,4-phenylenevinylene] and an electron transport material', pp. 1283–1285. Copyright (2004) American Institute of Physics. (b) Energy band diagram showing charge transfer from DFD to the MEH-PPV emissive polymer.

Other OLED Issues

- **Multifunctional** molecule/polymer
- Use of **energy transfer** (host-guest system); particularly useful for the red emitter system
- **White OLED**
- **Full-Color** Display Systems

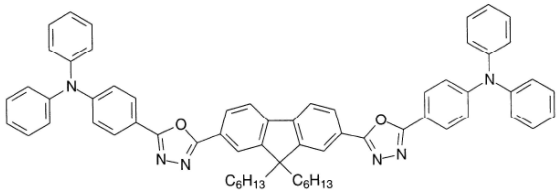

Figure 9.29 2,7-Bis[2-(4-diphenylaminophenyl)-1,3,4-oxadiazol-5-yl]-9,9-dihexylfluorene: molecule for OLEDs containing electron transport, hole transport and emissive groups [43].

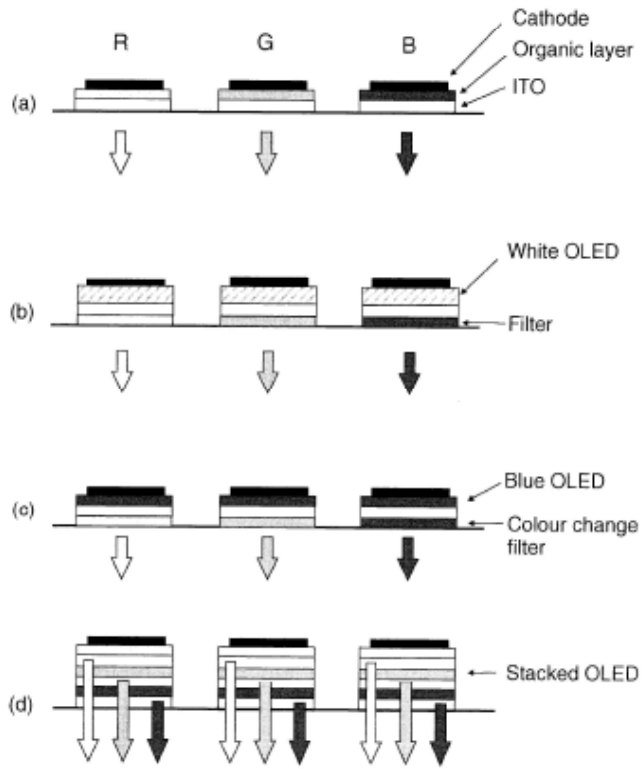

Figure 9.30 Schemes for generating full-colour displays. (a) Separate red, green and blue emitters (R, G and B) providing pixels side-by-side. (b) The light from white-emitting OLEDs is filtered to provide R, G and B emission. (c) The light from blue-emitting OLEDs is used to generate R, G and B emission through colour changing filters. (c) Stacked OLEDs emit R, G and B [36].

Fundamentals of PV

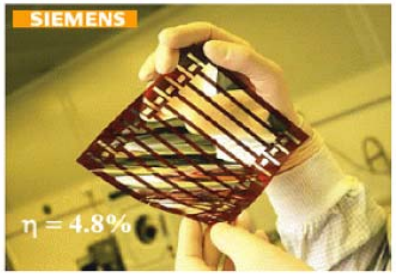

- Inorganic PV: e & h generated within, or close to, the **depletion region** and they would be free to migrate to opposite electrodes
- Organic PV: strong **exciton binding energy** (e & h bound), **small exciton diffusion length**– exciton diffusion to and dissociation at the Schottky barrier, or p-n heterojunction

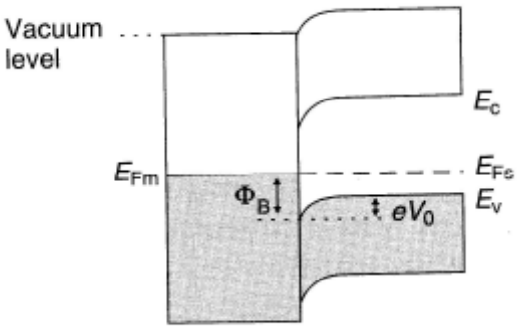

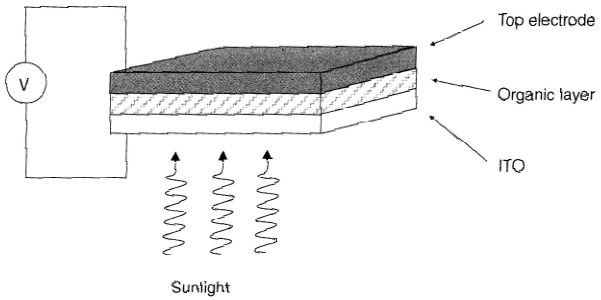

Figure 9.31 Schematic diagram showing the structure of a photovoltaic cell based on a conductive organic compound.

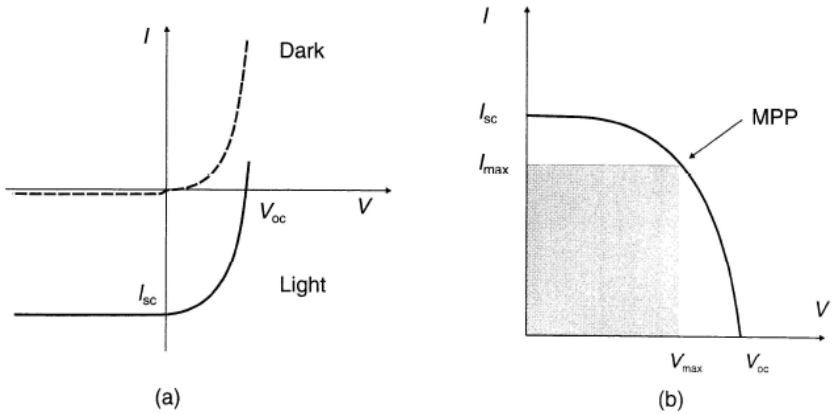

Figure 9.32 (a) Current I versus voltage V characteristics for an organic PV structure in the dark and in the light. V_{oc} = open-circuit voltage; I_{sc} = short-circuit current. (b) Expanded region of I–V curve showing the maximum voltage V_{max} and the maximum current I_{max} available from the solar cell. The shaded area represents the maximum power available from the cell. MPP = maximum power point.

$$\eta = \frac{I_{max} V_{max}}{P_i A} = \frac{I_{sc} V_{oc} F}{P_i A}$$

Low efficiency obtained for organic Schottky device !!

Organic Heterojunction PV

C. W. Tang, *Appl. Phys. Lett.*, **48**, 183 (1986)

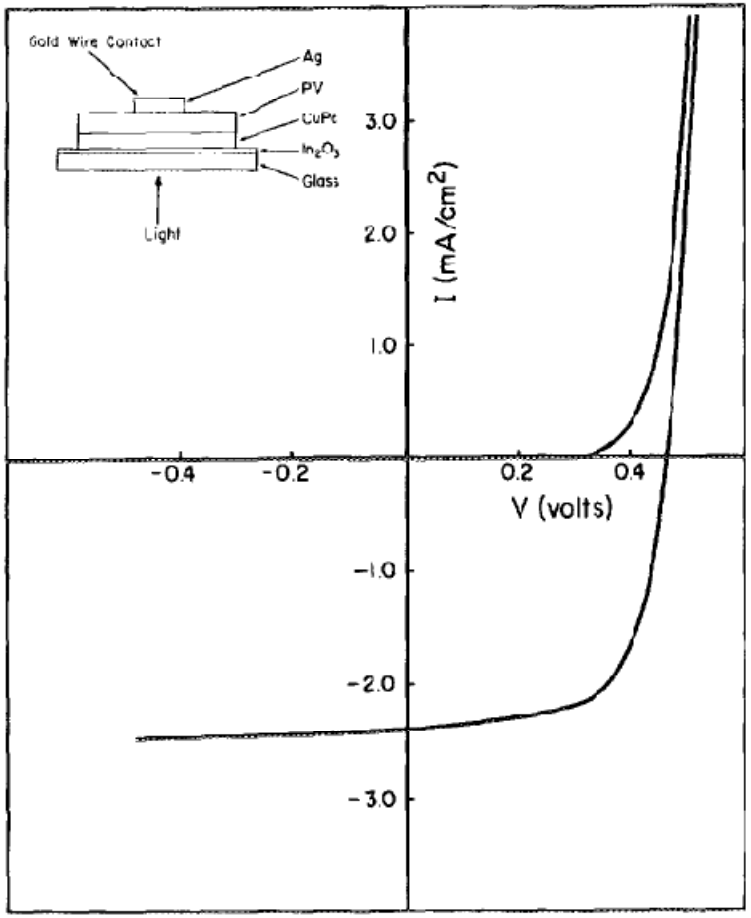

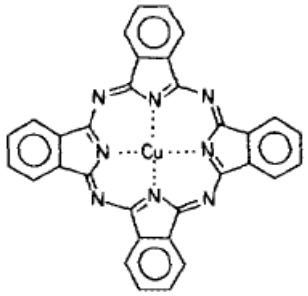

CuPc

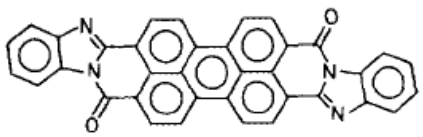

PV

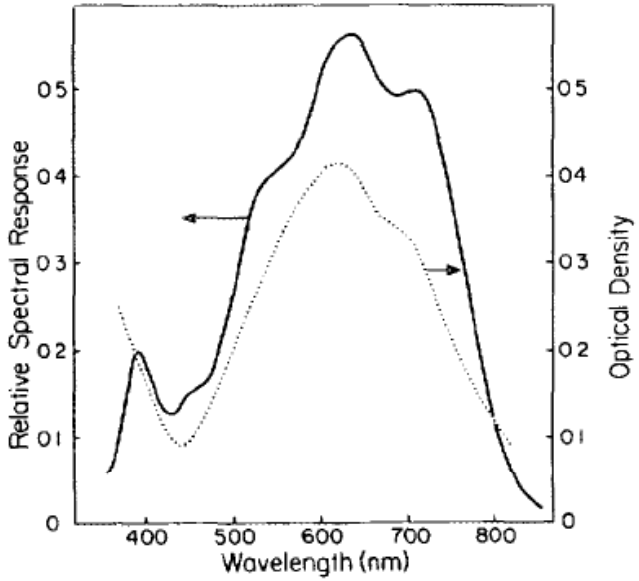

ITO/CuPc(30 nm)/PV(50 nm)/Ag

Two layer structure

V_{OC} = 450 mV, I_{SC} = 2.3 mA/cm^2, ff = 0.65, **η** = 0.95 %

Unit Processes for PV

- **Exciton binding energy** (E_g-E_{ex}): 0.1-0.2 eV for organic molecules
- Conditions for **CT**: $E_{ex}>I_{pd}-\chi_{EA}$
- Exciton **diffusion**: via Dexter & Föster ET

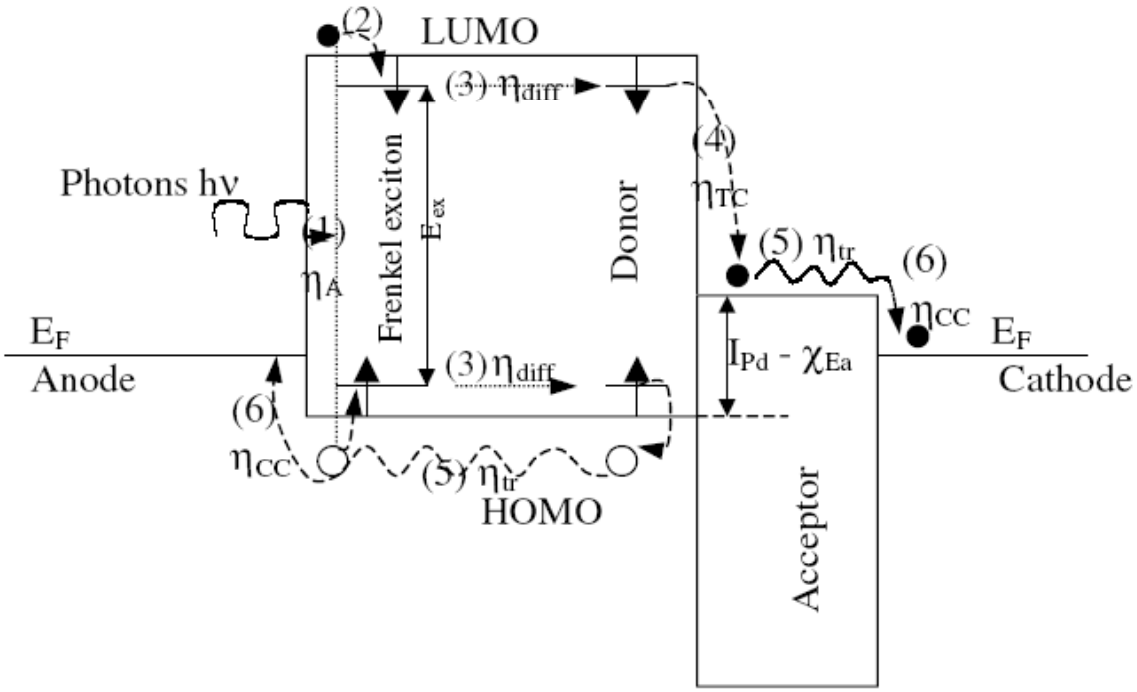

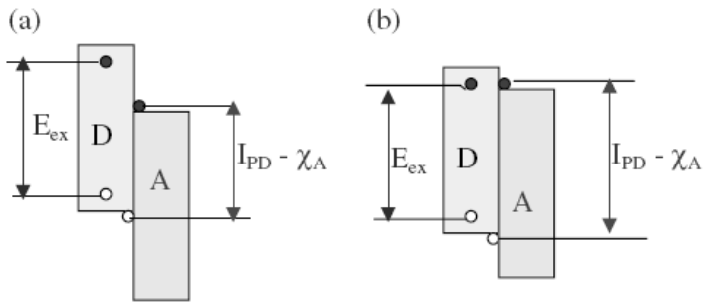

Figure 8. Condition for charge transfer: (a) allowed; and (b) forbidden.

A. Moliton and J.-M. Nunzi, *Polym. Int.*, **55**, 583 (2006)

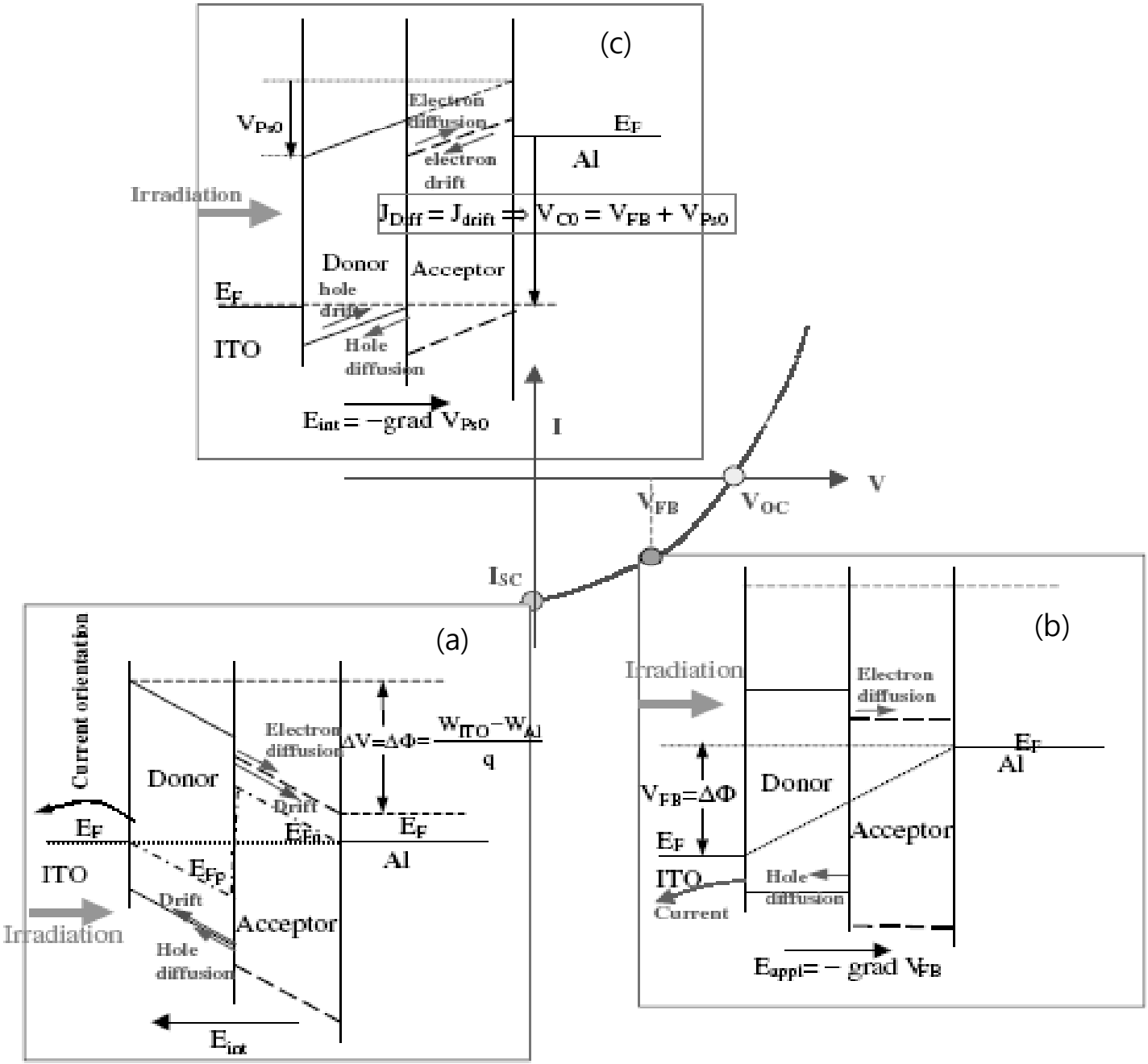

A. Moliton and J.-M. Nunzi, *Polym. Int.*, **55**, 583 (2006)

Organic Bulk Heterojunction for PV

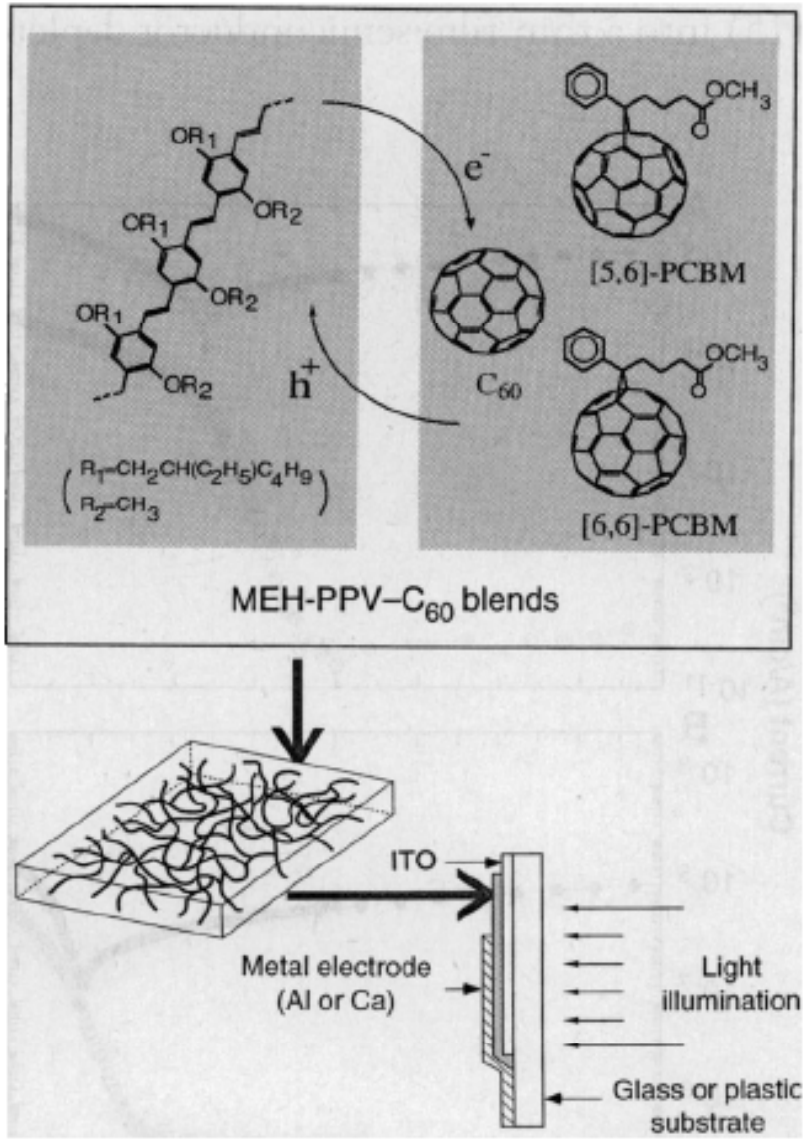

G. Yu, **A. J. Heeger** et. al., *Science,* **270**, 1789 (1995)

ITO/MEH-PPV:PCBM(1:4)/Ca

under 20 mW/cm^2 at 430 nm
η_e = 2.9 % (energy conversion efficiency)

Fig. 1. Schematic diagram of the photoinduced charge transfer process in MEH-PPV:C_{60} D-A blends. The structures of the two soluble C_{60} derivatives used in this study (denoted as [6,6]PCBM and [5,6]PCBM) are included. When cast as a film, the D and A species phase-separate into a bicontinuous network (bulk heterojunction material), as shown schematically. The structure of the photovoltaic cell fabricated with this bulk heterojunction material is sketched at the bottom.

Morphology Control for PV

- **A. J. Heeger** et al., Adv. Funct. Mat., 15, 1617 (2005)
- ITO/PEDOT/**P3HT:PCBM=1:0.8**/LiF/Al
- Under 80 mW/cm2, **η=~5%** post annealing at 150°C for 30 min

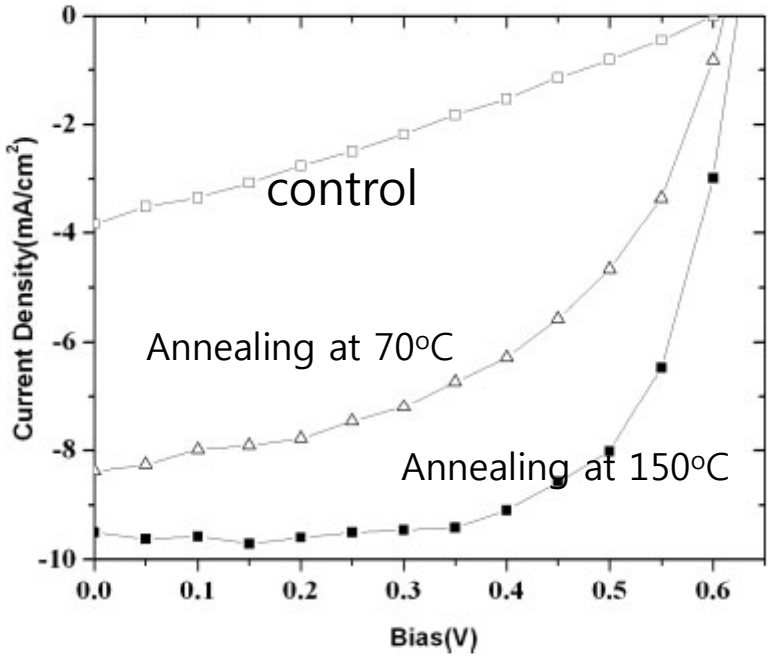

Figure 1. *I–V* curves obtained from P3HT:PCBM solar cells under AM 1.5 illumination at an irradiation intensity of 80 mW cm^{-2}. Devices without thermal annealing (open squares), devices with postproduction heat treatment at 70°C (open triangles), and devices with postproduction heat treatment at 150 °C (filled squares). All devices were annealed for 30 min. The device structure is ITO/PEDOT/P3HT:PCBM/Al.

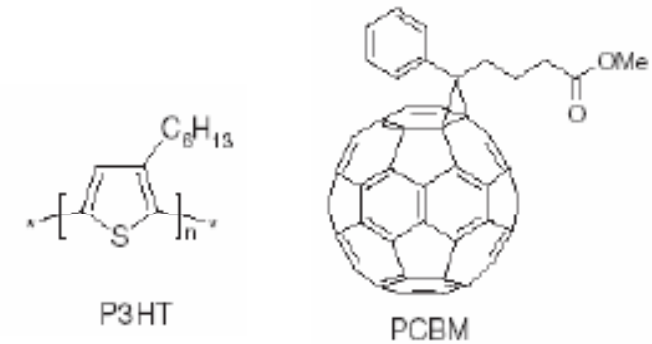

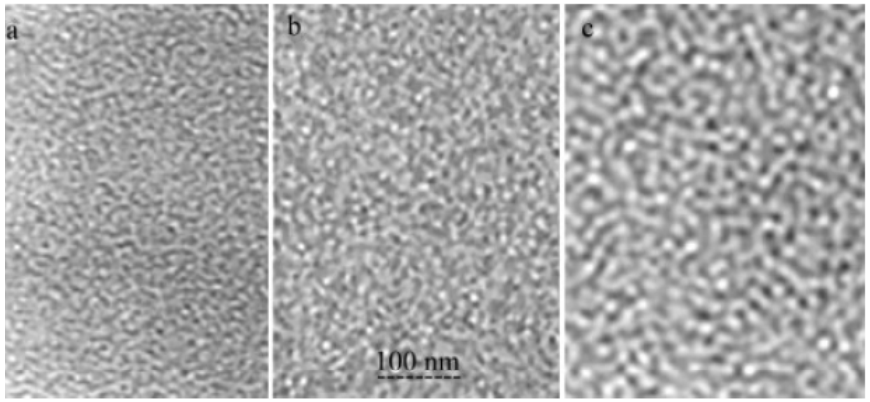

gure 3. TEM images of P3HT:PCBM film bulk morphology before thermal annealing (a), after ermal annealing at 150 °C for 30 minutes (b), and after thermal annealing at 150 °C for 2 h (c).

Efficient Tandem Polymer Solar Cells Fabricated by All-Solution Processing

Science, **317**, 222 (2007)

Jin Young Kim,[1,2] Kwanghee Lee,[1,2*] Nelson E. Coates,[1] Daniel Moses,[1]
Thuc-Quyen Nguyen,[1] Mark Dante,[1] Alan J. Heeger[1]

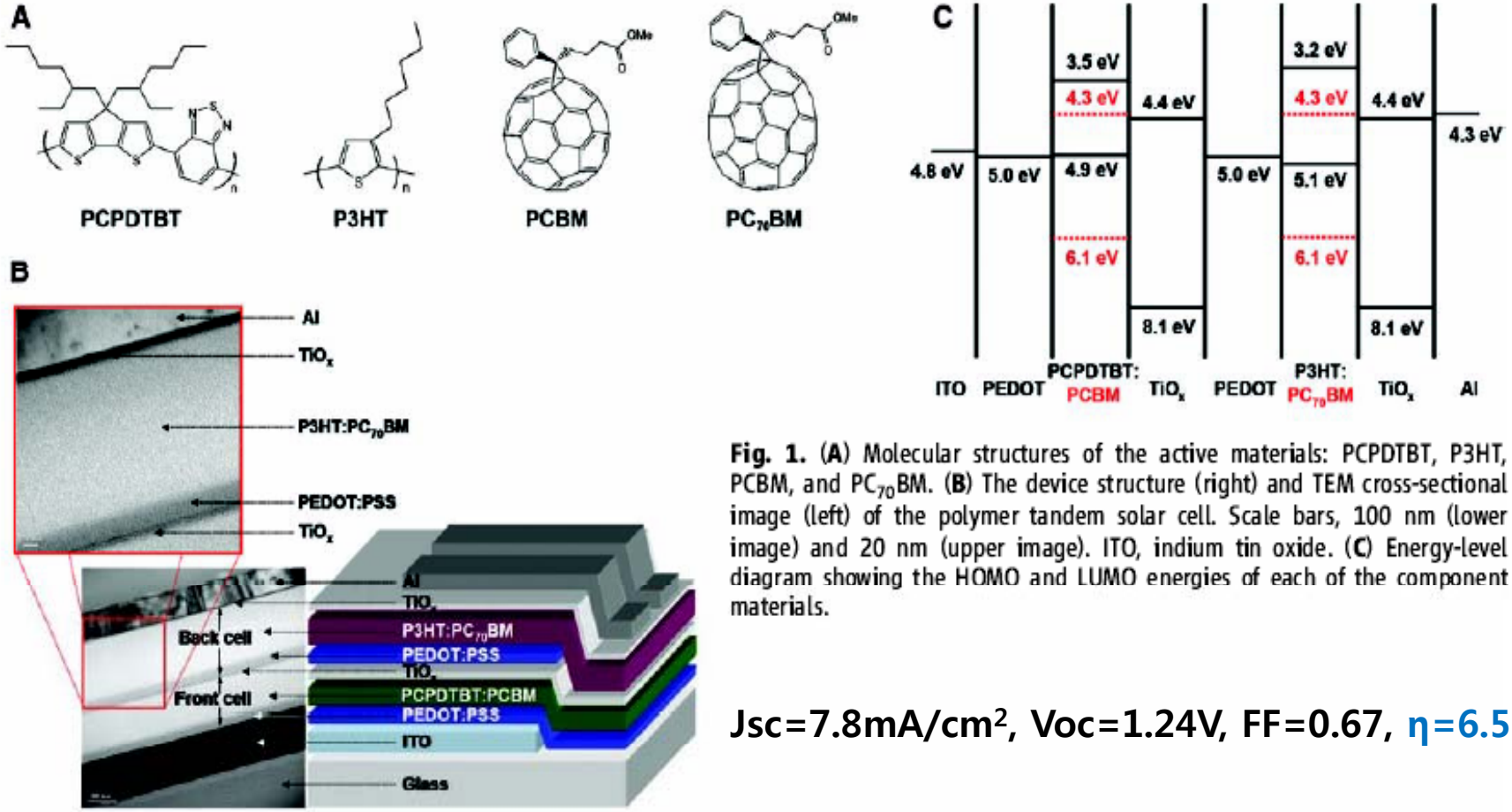

Fig. 1. (**A**) Molecular structures of the active materials: PCPDTBT, P3HT, PCBM, and $PC_{70}BM$. (**B**) The device structure (right) and TEM cross-sectional image (left) of the polymer tandem solar cell. Scale bars, 100 nm (lower image) and 20 nm (upper image). ITO, indium tin oxide. (**C**) Energy-level diagram showing the HOMO and LUMO energies of each of the component materials.

Jsc=7.8mA/cm^2, Voc=1.24V, FF=0.67, η=6.5%.

Design Rules for Efficient PV Donor

M. C. Scharber, A. J. Heeger, C. J. Brabec et. al., *Adv. Mater.,* **2006**, *18*, 789–794

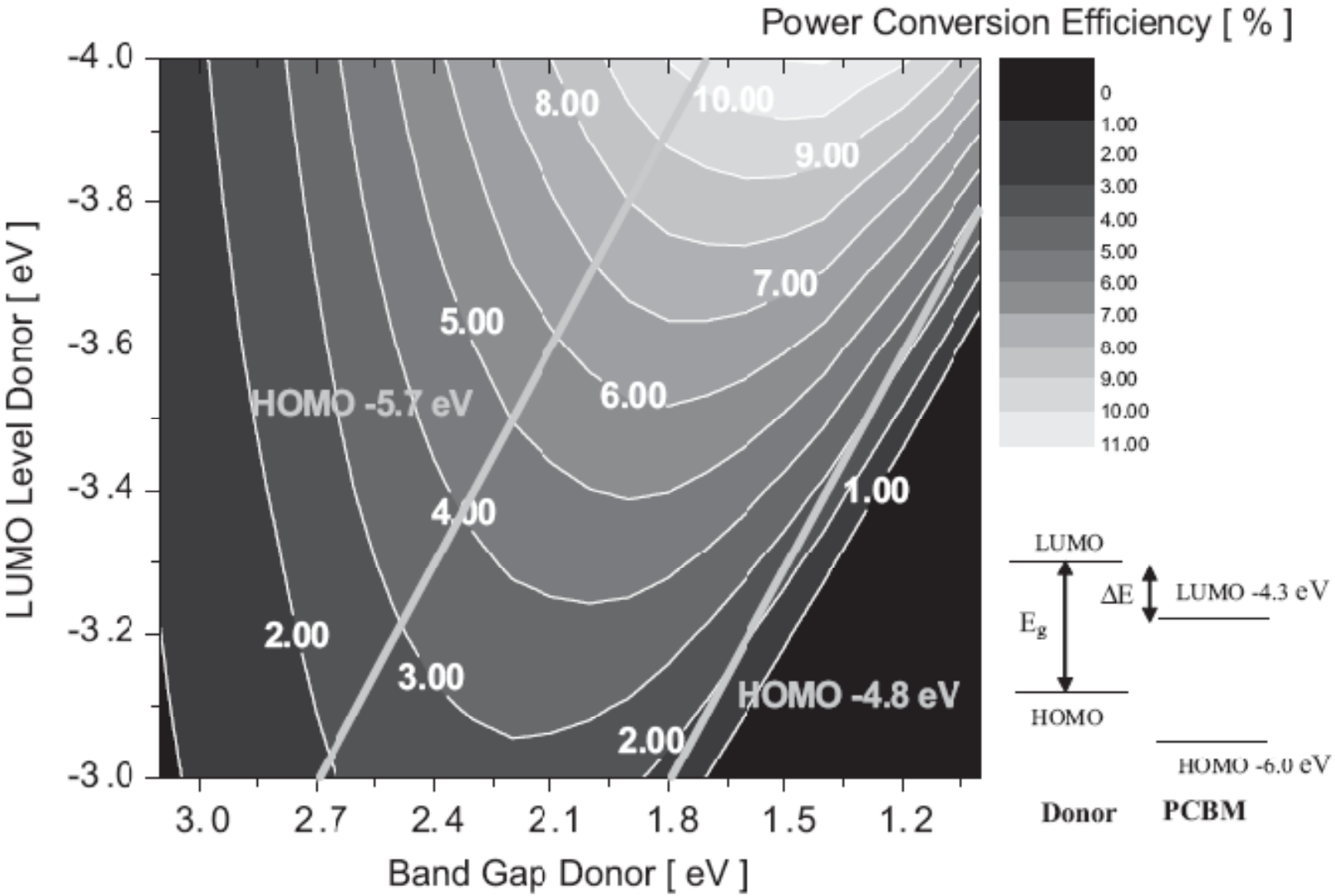

Dye-Sensitized Solar Cell

- **Grätzel** et al., *Nature*, 353, 737 (1991): nanoparticle TiO_2/Dye 7.1~7.9 % efficiency
- Recent Research Works: (1) Replacing the liquid electrolyte with gel or hole-transporting polymer, (2) Replacing the Ru dye with organic dyes

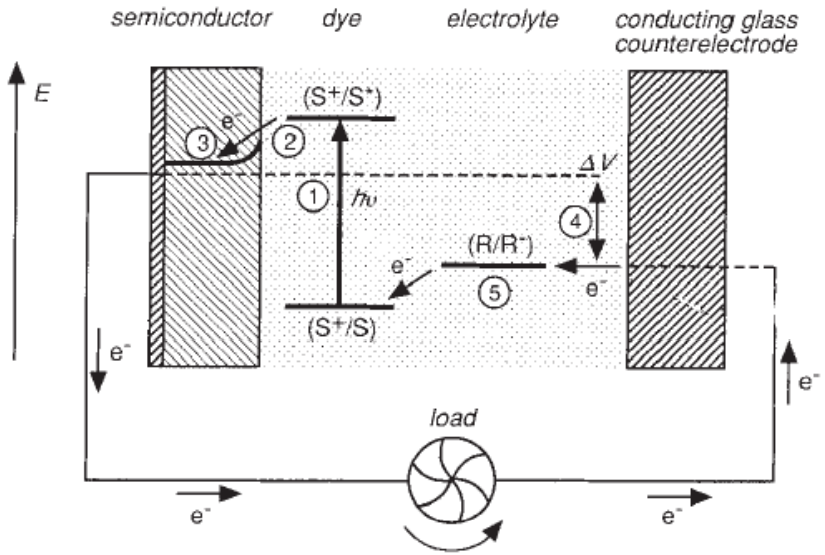

FIG. 1 Schematic representation of the principle of the dye-sensitized photovoltaic cell to indicate the electron energy level in the different phases. The cell voltage observed under illumination corresponds to the difference, ΔV, between the quasi-Fermi level of TiO_2 under illumination and the electrochemical potential of the electrolyte. The latter is equal to the Nernst potential of the redox couple (R/R^-) used to mediate charge transfer between the electrodes. S, sensitizer; S^*, electronically excited sensitizer; S^+, oxidized sensitizer.

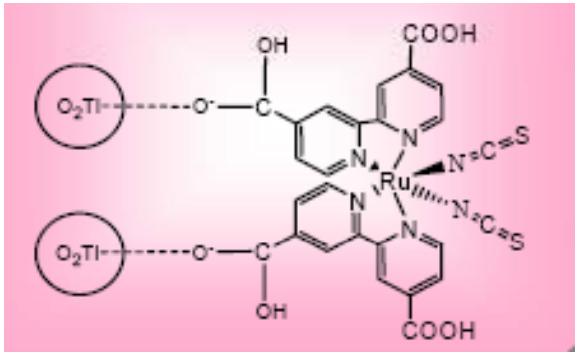

Xerography (Electrophotography)

- 1940 patented by C. F. Carlson

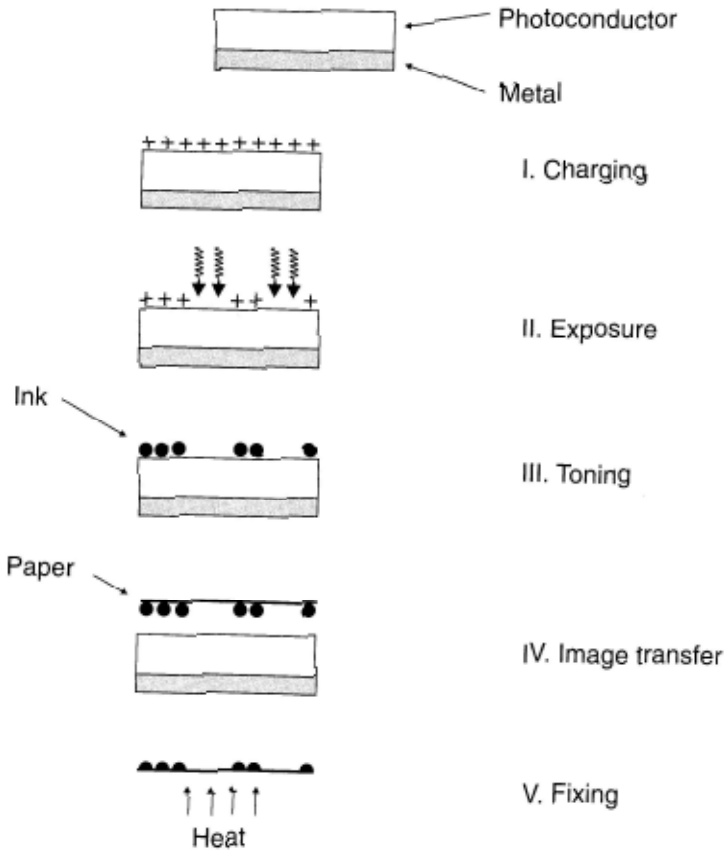

Figure 9.39 The important processing steps in xerography.

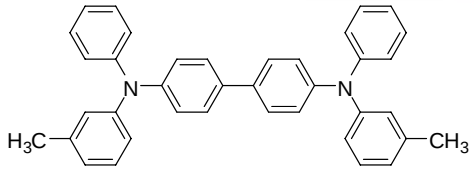

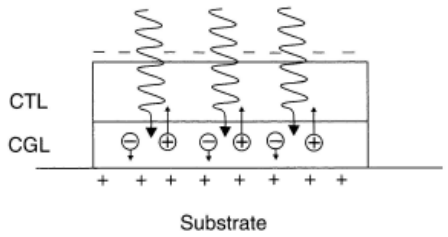

Figure 9.40 A two-layer xerographic material. CTL = charge-transport layer; CGL = charge generation layer.

Miscellaneous Plastic Electronics

- Conductive Coating : against antistatic and EM interference
- Li-Polymer Battery
- Fuel Cell Membranes
- Luminescent Concentrator for Solar Cell
- Organic Radical Battery
- Organic/Polymer Memory